FINITE ELEMENT BASED WEIGHT REDUCTION SUBJECT TO STABILITY CONSTRAINTS FOR AN AIRSHIP COMPOSITE DUCT

by

SOHAM M UMBRAJKAR

Presented to the Faculty of

The University of Texas at Arlington

in Partial Fulfillment of the Requirements

for the Degree of

MASTER OF SCIENCE IN MECHANICAL ENGINEERING

THE UNIVERSITY OF TEXAS AT ARLINGTON

MAY 2016

ABSTRACT

FINITE ELEMENT BASED WEIGHT REDUCTION SUBJECT TO

STABILITY CONSTRAINTS FOR AN AIRSHIP COMPOSITE DUCT

Soham M. Umbrajkar, M.S.

The University of Texas at Arlington, 2016

Supervising Professor: Dr. D. Stefan Dancila

The primary functions of High Altitude Long Endurance (HALE) airships are persistent observation and wide area direct line of sight communication. Traditional airships have an ellipsoidal type hull, which is characterized by a large aspect ratio but results in an increase in the weight of the envelope. In order to reduce the weight of an airship, a hull having lower aspect ratio would be preferred. A novel unconventional airship design having a toroidal geometry with a propulsive duct running from the front end to back end was developed by Dancila in an attempt to achieve this objective. The propulsive duct helps in reducing the drag associated with the toroidal shape by blowing of the wake region. The propulsive duct is subjected to hull pressure on its outer walls and airflow induced pressure on its inner walls. This results in in-plane duct wall compressive stress, which may potentially result in a loss of structural stability. In prior work a duct with sandwich composite configuration was investigated, to maintain an open duct, as it offers high specific stiffness, high specific strength and lightweight alternative to isotropic material construction. In this thesis a corrugated sandwich composite duct design is considered as it may provide a higher wall bending stiffness compared to a smooth duct. The results for the smooth sandwich composite duct obtained from the literature survey are used as a reference in this analysis. The duct is modeled and analyzed using the commercial finite element code ABAQUS. The objective is to reduce weight subject to stability constraints while maintaining a 50% margin of safety. There are two independent design parameters and one dependent design parameter for this analysis. The independent design parameters are the number of corrugation waves and amplitude of corrugation while the dependent parameter is the required thickness of

the foam to ensure stability. An FEM based method is used to reduce the weight of the corrugated duct design involving number of corrugation waves, amplitude of corrugation and foam thickness. The best configuration identified in this investigation provides a significant weight reduction of 32% compared to the baseline smooth duct.

TABLE OF CONTENTS

LIST OF ILLUSTRATIONS

Figure Page

LIST OF TABLES

CHAPTER 1

INTRODUCTION

1.1 Background

High Altitude Long Endurance (HALE) airships are platforms of interest for persistent observation and wide area direct line-of-sight communications due to their station keeping capabilities at high altitudes. The airship operates on the principle of buoyancy. The lift generated through buoyancy is proportional to the difference in density between surrounding fluid and the fluid enclosed in the hull, and the envelope volume. A single airship has the capability of covering by direct line of sight an area of 250-300 km effective radius from 19.82 km (65kft) altitude. When used for broadcasting and communication purposes they are an efficient competition for satellites and they also have low maintenance and operational costs.

To maximize the lift generated by a given volume of gas, the envelope area should be minimized. A sphere has a minimum surface area for a given volume, but spheres have bluff bodies and develop a high drag. Conventional airships consist of an ellipsoidal hull design, which results in lower drag but are aerodynamically instable. Such ellipsoidal shapes are characterized by larger envelope area, which is directly associated with weight. In order to reduce the weight, hull shapes with lower aspect ratio could be adopted which would cause the envelope surface area to decrease.

Meier *et al* [1] conducted experimental investigations on a smooth solid sphere consisting of a front-to-back duct to study the drag reduction by ventilation. A sphere having a relative duct diameter of 15% was investigated and the results showed over 60% reduction in drag.

Based on these results, Dancila [2] developed a novel unconventional HALE airship design having a toroidal configuration with a hull duct connecting the front and the back. The propulsive duct connecting the front and the back is subjected to a pressure difference enhancing the flow in the duct, which further helps in drag reduction by blowing of the wake region.

1.2 Motivation

Airships need to carry certain payloads in order to perform their tasks. A reduction in weight would lead to an increase in airship payload carrying capacity. The hull duct is subjected to hull overpressure on its outer surface and a flow induced pressure on its inner surface. This loading condition causes an in-plane compressive stress in the hull duct, which may cause a potential loss of stability. In order to keep the duct from collapsing and supporting the loads, an appropriate duct structure in needed. With a view to minimize weight, sandwich composite configurations are a good choice to proceed as shown by Khode [3] with her investigation of a smooth converging duct. Corrugated configurations provide a higher wall bending stiffness compared to a smooth configuration, which may lead to a decrease in weight of the duct subjected to lateral pressure with a 50% margin of safety.

1.3 Research Objectives

The research objectives of this work are to investigate the further weight reduction potential of corrugated configurations for sandwich composite construction subjected to stability constraints.

CHAPTER 2

LITERATURE SURVEY

A typical sandwich composite structure consists of high stiffness composite face sheets and a foam core having low density. Sandwich composite structures exhibit a higher bending stiffness and are lightweight. Due to these attributes they find extensive application in the aerospace and marine industry. Hao *et al* [4] showed that sandwich composite structures compared to homogenous material offered a higher stiffness and also a higher load carrying capability. Khode [3] conducted a weight minimization study for a smooth converging duct made up of foam-only, composite-only and sandwich composite setting using 0^0 and 90^0 ply orientations. For the sandwich composite duct one-ply, two-ply and three-ply sandwich configurations were investigated. The study revealed that the best possible minimum weight solution was provided by sandwich configuration and the optimum ply orientation would be always 90^0, which is intuitively consistent when considering the fibers run in the same direction as the hoop stress.

In this study we try to further build upon the results of Khode [3] by investigating a corrugated converging duct design. There are two independent parameters involved with a corrugated duct design. A weight reduction procedure was carried out using FEM-based method for the corrugated duct configurations.

CHAPTER 3

STRUCTURAL WEIGHT REDUCTION

3.1 FEM-Based Duct Stability Analysis

In this chapter we explore a methodology to optimize the design of a corrugated duct in order to obtain a reduced weight for the airship duct. The corrugated duct design depends on two parameters; a) number of corrugation waves along the length of the duct, b) amplitude of the corrugation. The objective is to obtain a corrugated configuration having lower weight than the baseline duct subject to lateral pressure, with a margin of safety of 50%.

The boundary conditions, operating conditions and loading conditions used in this analysis are same as used by Khode [3].

3.1.1 Geometric Configuration

The work done by Meier *et al* [1] showed a significant drag reduction for spheres having a relative duct of radius with 15%. The airship model investigated by Khode [3] has a radius of 20 m with a duct running from the front to the back. The airship model has a propeller situated at the center of the duct. The radius of duct at propeller would be 3 m. The dimensions of the duct are as shown in Table 3.1

Table 3.1 Geometric dimensions of airship

Geometric Feature	**Dimensions**
Radius of airship	20 m
Radius of duct at inlet	4.24 m
Radius of duct at propeller	3 m
Radius of duct at exit	2.12 m

Corrugation Shape Definition

The corrugated duct was modeled in ABAQUS by using geometric points derived from the Equation 4.1, where x' and r' (x') are shown in Figure 3.1

$$r'(x') = \frac{A}{2}[1 - \cos(\frac{2n\pi x'}{L'})] \qquad (4.1)$$

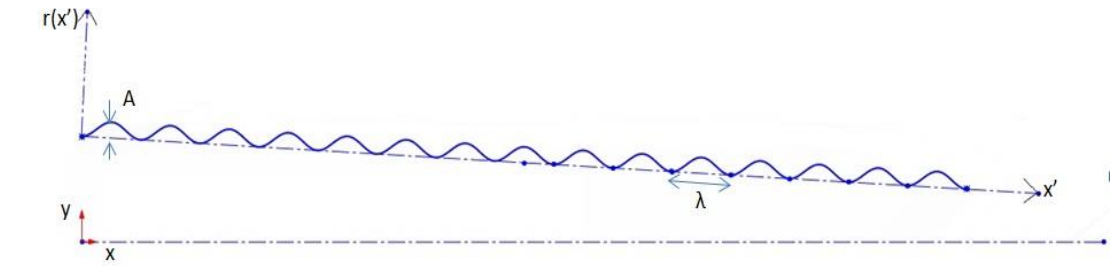

Figure 3.1 Geometry of corrugated converging duct

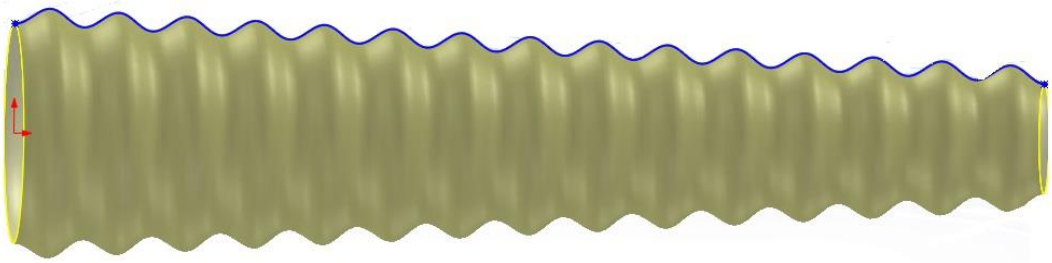

Figure 3.2 Corrugated duct with N=15; A=15%

3.1.2 Material Properties

The sandwich composite configuration consisted of fiber-reinforced composite face sheets and a foam core. The face sheets and core are assumed to be made up of graphite/epoxy (IM7/8552) having a 125μm cured ply thickness and H100 Divinycell foam respectively. The material properties of IM7/8552 and foam are given in Table 3.2 and 3.3, respectively.

Table 3.2 IM7/8552 material properties

E_{11}	155.0 GPa
E_{22}	12.10 GPa
E_{33}	12.10 GPa
ν_{23}	0.458
ν_{13}	0.248
ν_{12}	0.248
G_{23}	4.15 GPa
G_{13}	4.40 GPa
G_{12}	4.40 GPa
ρ	1590 kg/m^3

Table 3.3 H100 Divinycell foam

E	111.10 MPa
ν	0.1
ρ	100 kg/m^3

3.1.3 Operating Conditions for Airship

The sandwich composite structure was optimized for the airship operating at sea level. The atmospheric properties such as wind speed, pressure and density at sea level are known and given in Table 3.4

Table 3.4 Atmospheric properties at sea level

Atmospheric Parameter	**Value**
Pressure	101,325 Pa
Density	1.225 kg/m^3
Velocity	20 m/s

3.1.4 Applied Load

The corrugated converging duct is subjected to hull overpressure on its outer surface and flow induced pressure on its inner surface. The net pressure acting on the duct is going to be difference of the hull overpressure of 200 Pa and the pressure induced due to the flow, which is a function of position along the duct as shown in Figure 3.3. Khode [3] developed the net pressure distribution on a duct as function of position of the duct using the actuator disk theory [5]. The lateral pressure applied on the duct is shown in Figure 3.4, for which ABAQUS would determine the factor of safety of 1.5.

Pressure at front of propeller at sea level

$$P_{front} = 45 - \frac{61353.6}{(0.000454951y^2 - 0.0712311y + 4.24264)^4} \quad \text{..... (3.1)}$$

Pressure at back of propeller at sea level

$$P_{rear} = 1351.67 - \frac{61353.6}{(0.000454951y^2 - 0.0712311y + 4.24264)^4} \quad \text{..... (3.2)}$$

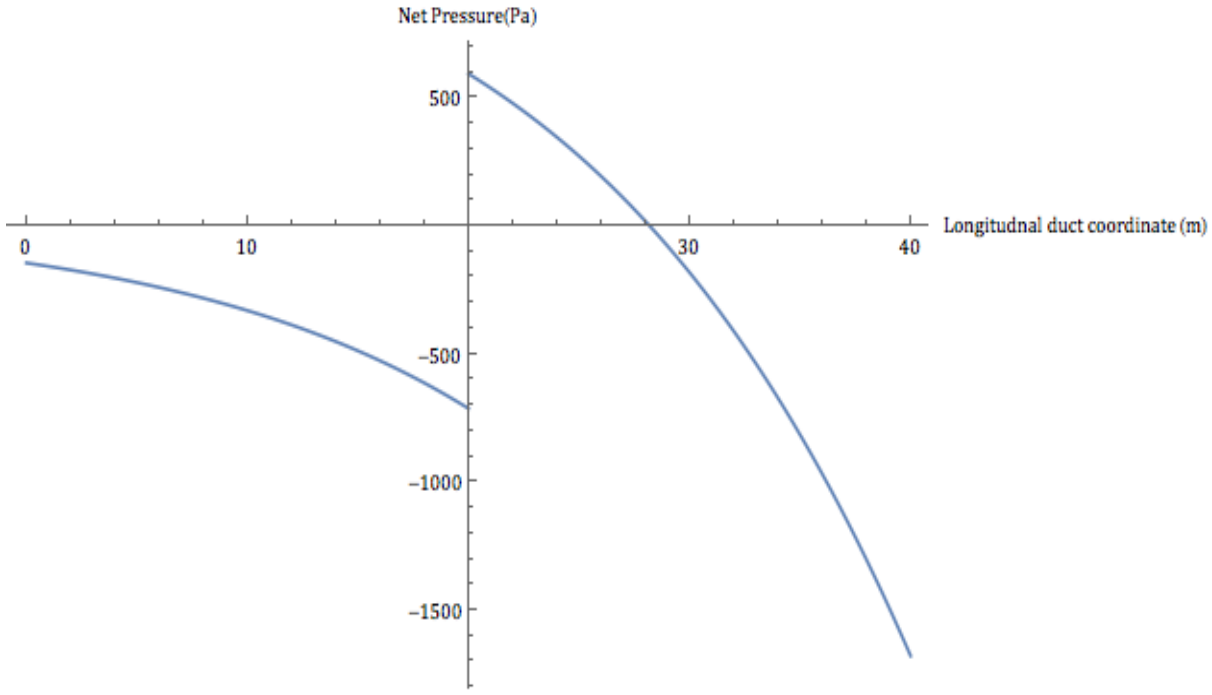

Figure 3.3 Net pressure acting on the converging duct at sea level

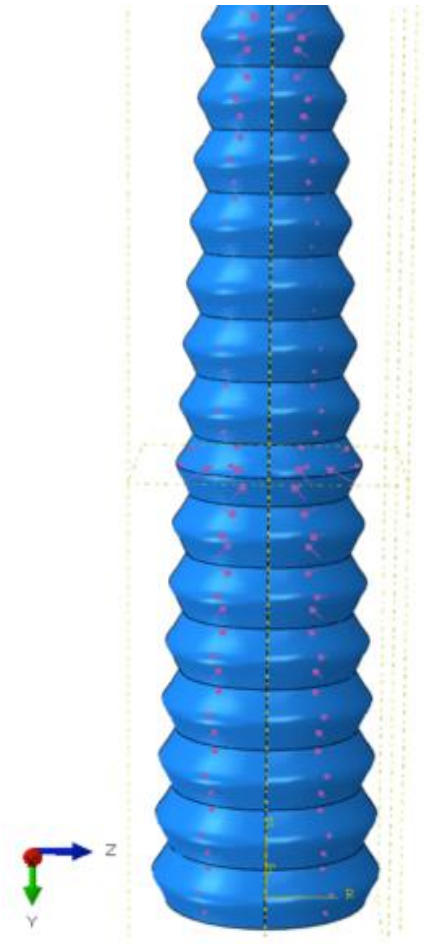

Figure 3.4 Net pressure distribution along the corrugated duct with N=15; A=15%

3.1.5 Boundary Conditions

In order to impose a free-free boundary condition in the FEM code under the action of lateral pressure, it is necessary to prevent the rigid body motion. This can be achieved by constraining all six rigid body degrees of freedom of the corrugated duct as shown in Figure 3.5. The free-free boundary condition is achieved by imposing the constraints given in Table 3.5

Table 3.5 Boundary conditions to prevent rigid body motion

Position	Constrained degrees of freedom	Effect
90^0	U1, U2	No translation in the global X and Y direction
0^0	U2. U3	No translation in global Z direction and no rotation about the global Z axis
270^0	U1, U2	No rotation about the global X and Y axis

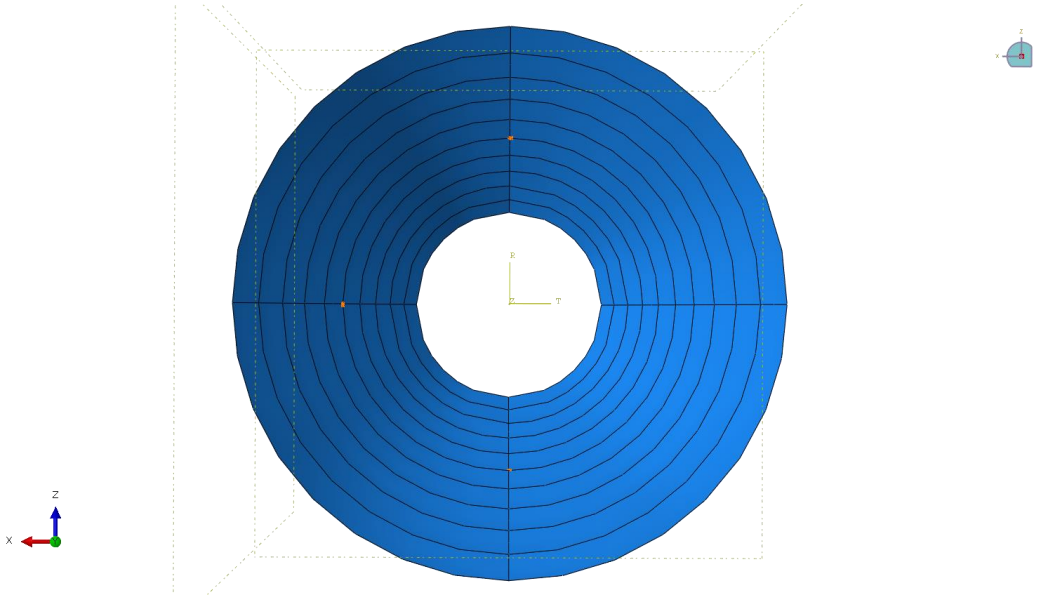

Figure 3.5 Boundary conditions

3.1.6 Meshing

For the purpose of this analysis, the S8R element is used. The S8R are doubly curved, thick shell elements having 8 nodes with a quadratic shape function that captures the transverse shear behavior. Based on the algorithm used by the FEM code ABAQUS, it is necessary for the neighboring shell element normals at the nodes to lie within 20^0 of each other in order to capture the curvature of the body accurately and to provide an accurate solution. If the angle subtended

by shell element normals is greater than 20^0, then ABAQUS introduces a fold/thick line. As the amplitude of the wave increases, the radius of curvature decreases making it necessary to have more elements along the curvature of the wave to obtain accurate results. The aspect ratios of the element in regards to all dimensions are maintained within the ratio 10:1. Configurations having a low radius of curvature would need more elements to satisfy the 20^0 constraints and meet the aspect ratio requirement.

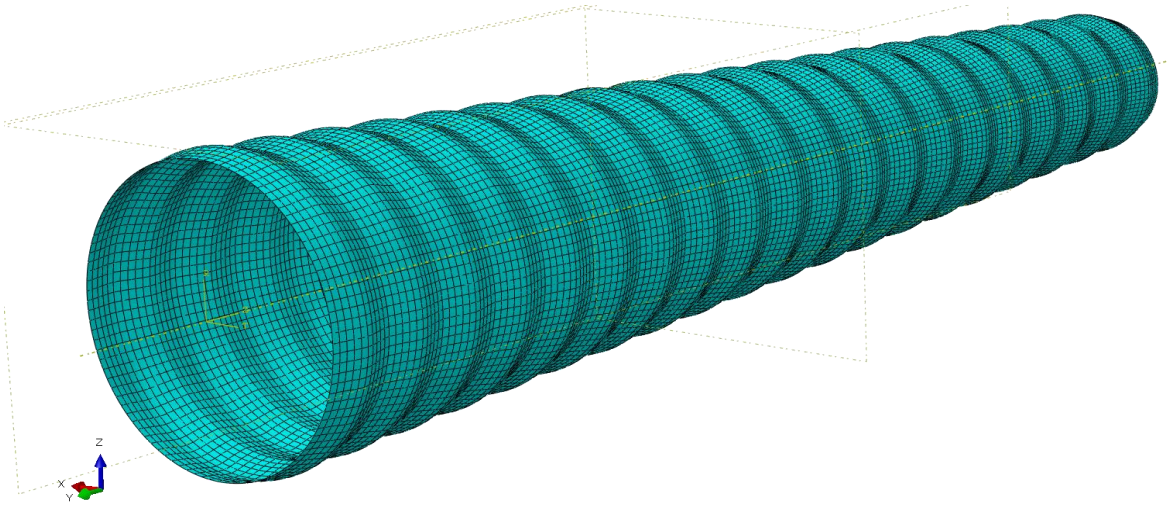

Figure 3.6 Mesh for corrugated duct with N=20; A=5%

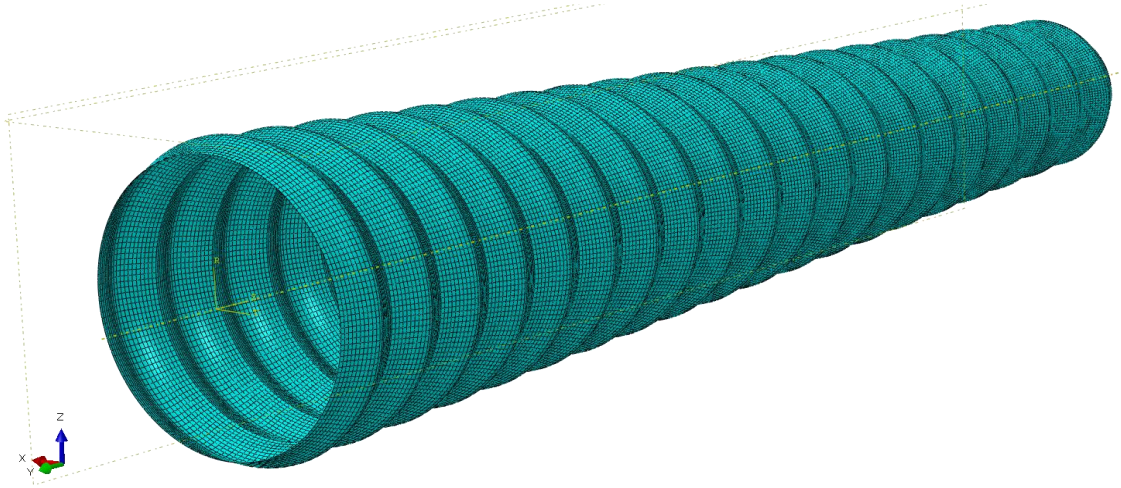

Figure 3.7 Mesh for corrugated duct with N=20; A=10%

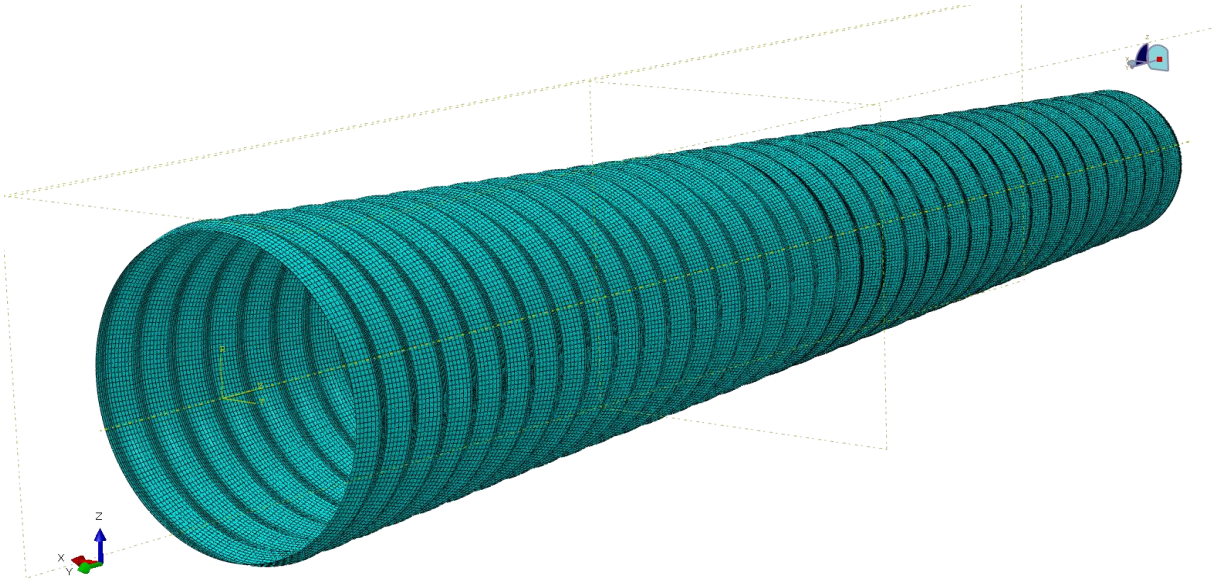

Figure 3.8 Mesh for corrugated duct with N=45; A=5%

3.1.7 Results and Discussions

Table 3.6 Result comparisons

LayUp	Weight obtained by Khode(kgf)	Weight (kgf)	% Difference
[90/F/90]	2147.550	2224.64	3.58
[0/F/0]	5182.100	5375.72	3.73
[0_2/F/0_2]	4607.880	4784.41	3.83
[90_2/F/90_2]	1905.960	1959.99	2.83

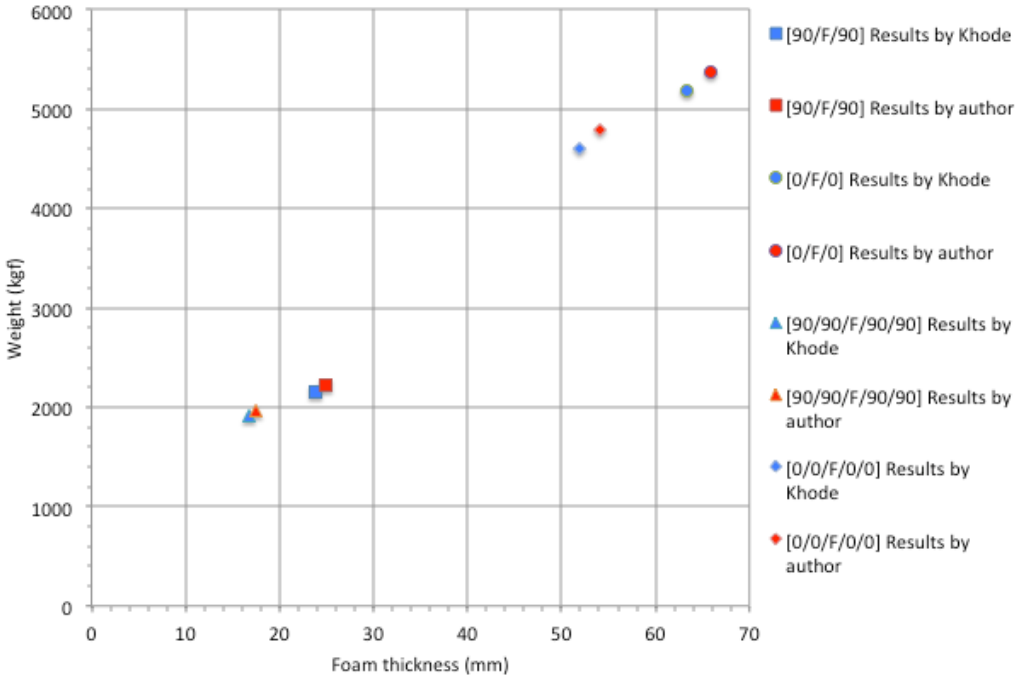

Figure 3.9 Comparison of results

The results obtained by this author were within 4% of the results obtained by Khode [3]. Considering corrugated construction to investigate further, a potential reduction in weight of the airship duct for a [90_2/F/90_2] layup.

3.2 Structural Weight Reduction of Sandwich Composite Duct at Sea Level Condition

A parametric study for a corrugated sandwich composite configuration involving two independent design parameters was performed: (a) number of waves along the length of the duct, (b) amplitude of the wave as percentage of radius at inlet. For a certain number of waves, the amplitude was varied and the required foam thickness for that configuration was determined. An interpolation function was used to find the required foam thickness corresponding to a factor of safety of 1.5. The interpolation function was determined by making three initial guesses for the foam thickness. ABAQUS was then used to solve for the factor of safety for those three values of foam thickness. A quadratic function was found based on those three points, which was solved for required foam thickness for a factor of safety of 1.5. The weight of the corrugated duct

depends on the thickness of the foam and lateral area of the duct. For a certain number of waves the amplitude of corrugation was increased until the weight of the latest configuration exceeded the weight of the previous configuration. If this condition was satisfied then the analysis for that number of waves was stopped. Further analysis was performed by increasing the number of waves and varying the amplitude for this new configuration of waves.

3.2.1 Design of Corrugated Sandwich Composite Duct

A design study was performed in ABAQUS for a two-ply sandwich composite layup with the number of corrugated waves and amplitude as given in Table 3.7. The values of the weight of the corrugated duct and foam thickness obtained in this analysis are normalized with respect to the weight and foam thickness values for a smooth duct obtained by this author for a $[90_2/F/90_2]$ layup (Table 3.7).

Table 3.7 Corrugated Configurations

Number of waves	**Amplitude (%r_i)**
10	5
	10
	15
15	5
	10
	15
20	5
	7
	12
	15
25	5
	7
	10
30	5
	6
	7
	8
	10
35	5
40	5
45	5
50	5
55	5
60	5

3.2.1.1 Configuration for N=10

Table 3.8 Results for N=10

Number of waves	Amplitude	Normalized foam thickness	Normalized Weight
10	5	1.070	1.131
	10	0.953	1.099
	15	0.926	1.148

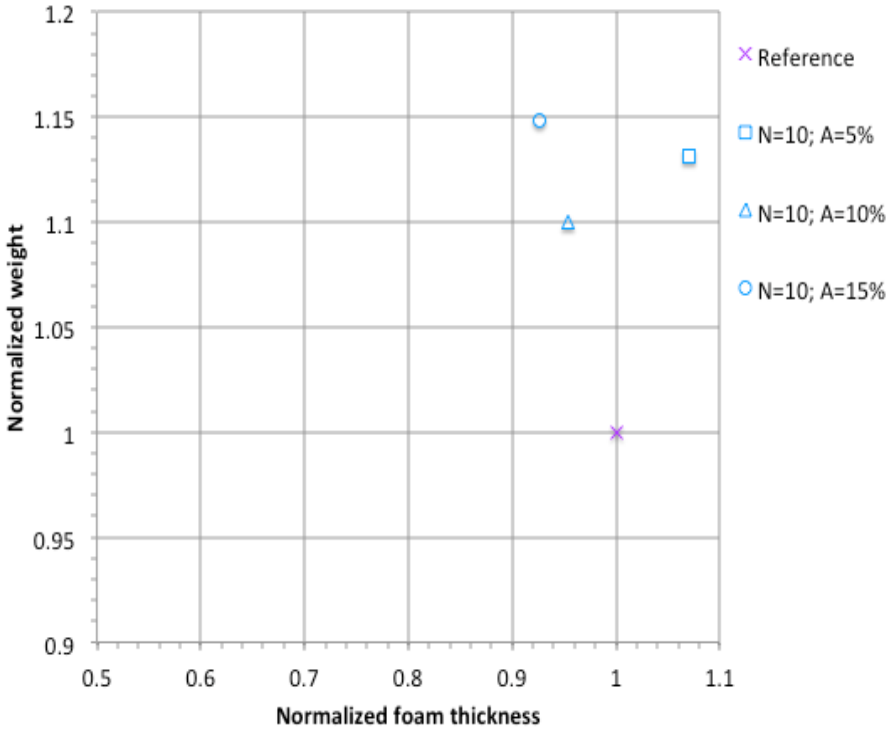

Figure 3.10 Normalized weight vs normalized thickness for N=10

The normalized thickness and normalized weight for N=10 are shown in Figure 3.10. We observe that for this configuration the weight of corrugated converging duct is not lower compared to a smooth converging duct.

The weight of the duct is a function of the lateral surface area and the thickness of the foam. As the thickness of the foam decreases for N=10 there is an increase in the area of

corrugated duct. The combined effect of the area and thickness does not result in a weight lower than that of a smooth duct, hence we proceed by increasing the number of waves.

3.2.1.2 Configuration for N=15

Table 3.9 Results for N=15

Number of waves	Amplitude	Normalized foam thickness	Normalized Weight
15	5	0.912	1.022
	10	0.750	0.971
	15	0.755	1.070

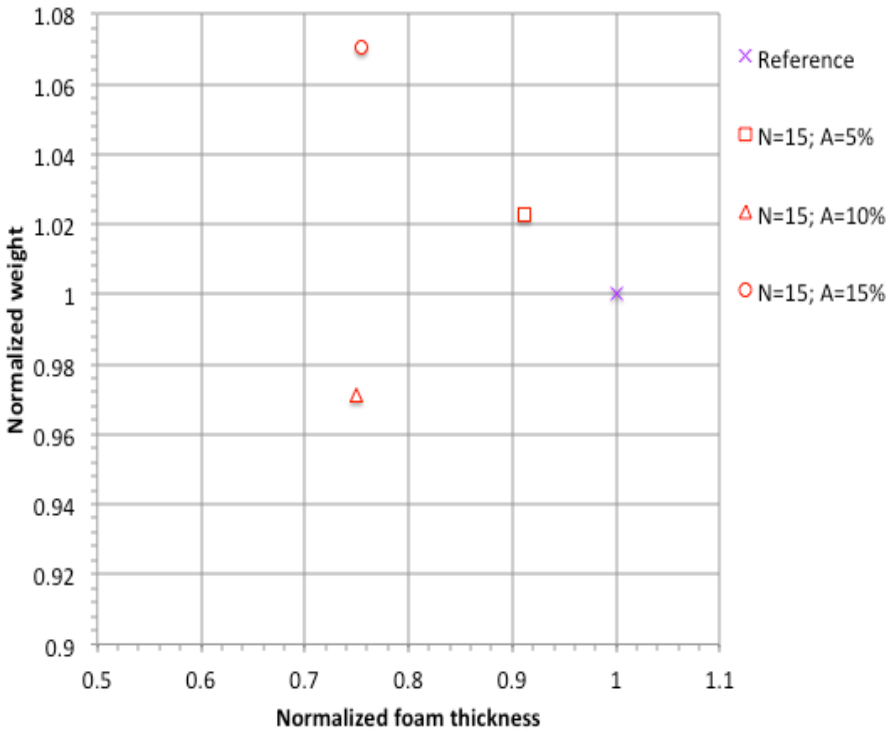

Figure 3.11 Normalized weight vs normalized thickness for N=15

3.2.1.3 Configuration for N=20

Table 3.10 Results for N=20

Number of waves	Amplitude	Normalized foam thickness	Normalized Weight
20	5	0.816	0.962
	7	0.676	0.888
	12	0.667	0.988
	15	0.708	1.108

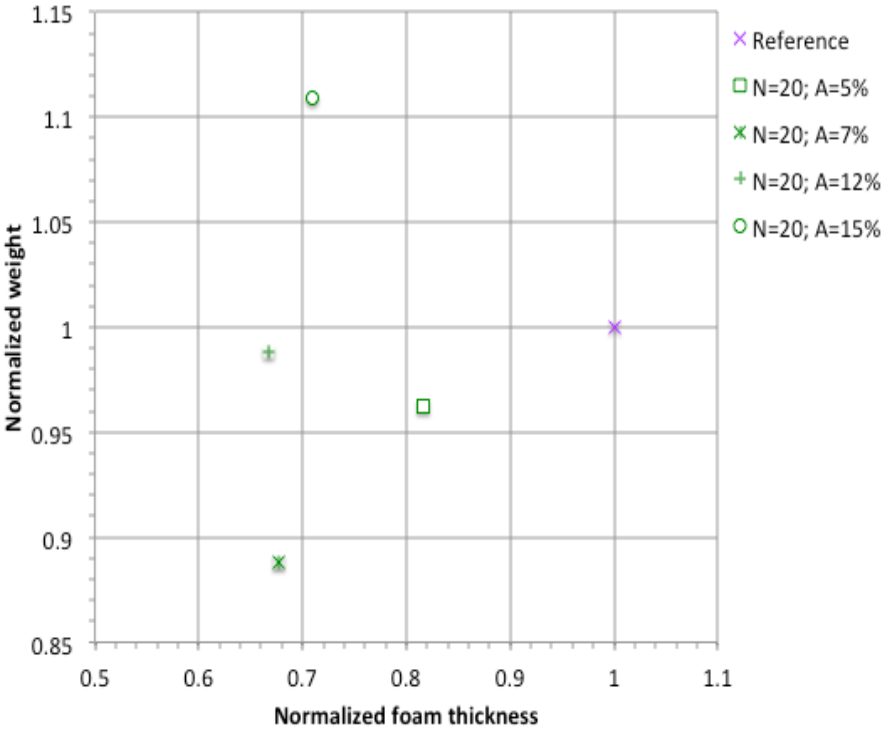

Figure 3.12 Normalized weight vs normalized thickness for N=20

3.2.1.4 Configuration for N=25

Table 3.11 Results for N=25

Number of waves	Amplitude	Normalized foam thickness	Normalized Weight
25	5	0.662	0.857
	7	0.563	0.820
	10	0.612	0.937

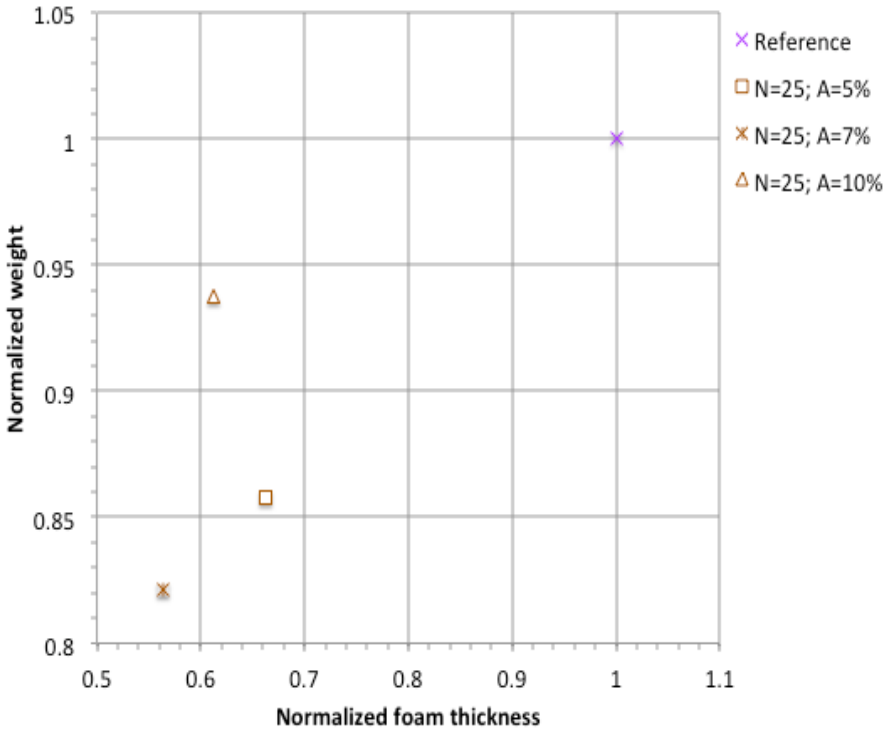

Figure 3.13 Normalized weight vs normalized thickness for N=25

3.2.1.5 Configuration for N=30

Table 3.12 Results for N=30

Number of waves	Amplitude	Normalized foam thickness	Normalized Weight
30	5	0.548	0.783
	6	0.498	0.765
	7	0.487	0.781
	8	0.531	0.847
	10	0.564	0.942

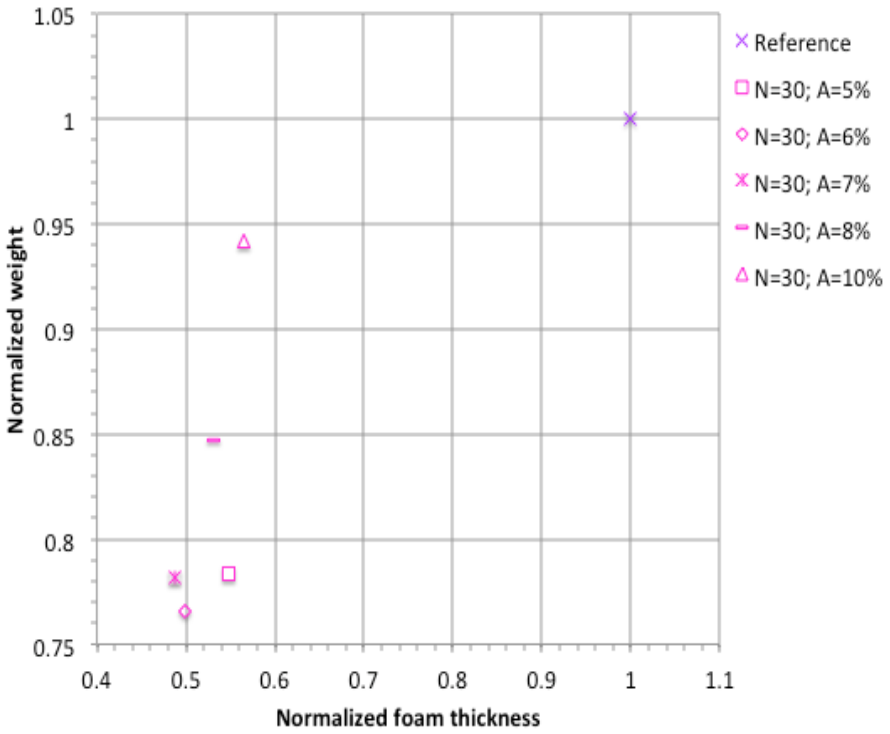

Figure 3.14 Normalized weight vs normalized thickness for N=30

3.2.1.6 Configurations for A=10% and A=15%

Table 3.13 Results for A=10% and A=15%

Amplitude	Number of waves	Normalized foam thickness	Normalized Weight
10	10	0.953	1.099
	15	0.750	0.971
	25	0.612	0.937
	30	0.564	0.942
15	10	0.926	1.148
	15	0.755	1.070
	20	0.708	1.108

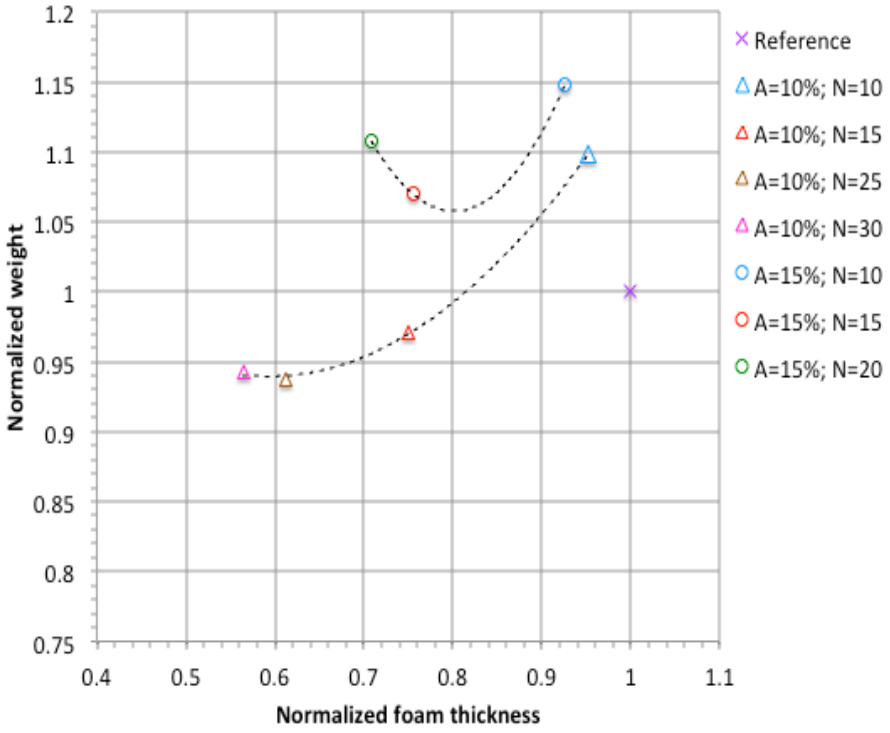

Figure 3.15 Normalized weight vs normalized thickness for A=10% and A=15%

The results for normalized thickness vs normalized weight for A=10% and A=15% are shown in Figure 3.15. For these configurations as the number of waves increases the weight

starts decreasing until it reaches the minimum point, after which a further increase in number of waves results in an increase in weight. The minimum weight obtained for A=15% is higher compared to the minimum weight obtained for A=10%.

This response suggests that in order to achieve a further reduction in weight for a corrugated duct, a configuration involving a higher number of waves with low amplitude should be explored.

Hence the further analysis is continued by increasing the number of waves for A=5% to find the weight of the corrugated duct when subjected to a lateral pressure with a margin of safety of 50%

3.2.1.7 Configuration for A=5% with increasing number of waves

As discussed in the previous section, we proceed with configuration having lower amplitude and a higher number of waves.

Table 3.14 Results for A=5

Amplitude	Number of waves	Normalized foam thickness	Normalized Weight
5	35	0.458	0.726
	40	0.393	0.689
	45	0.367	0.683
	50	0.339	0.675
	55	0.317	0.673
	60	0.294	0.670

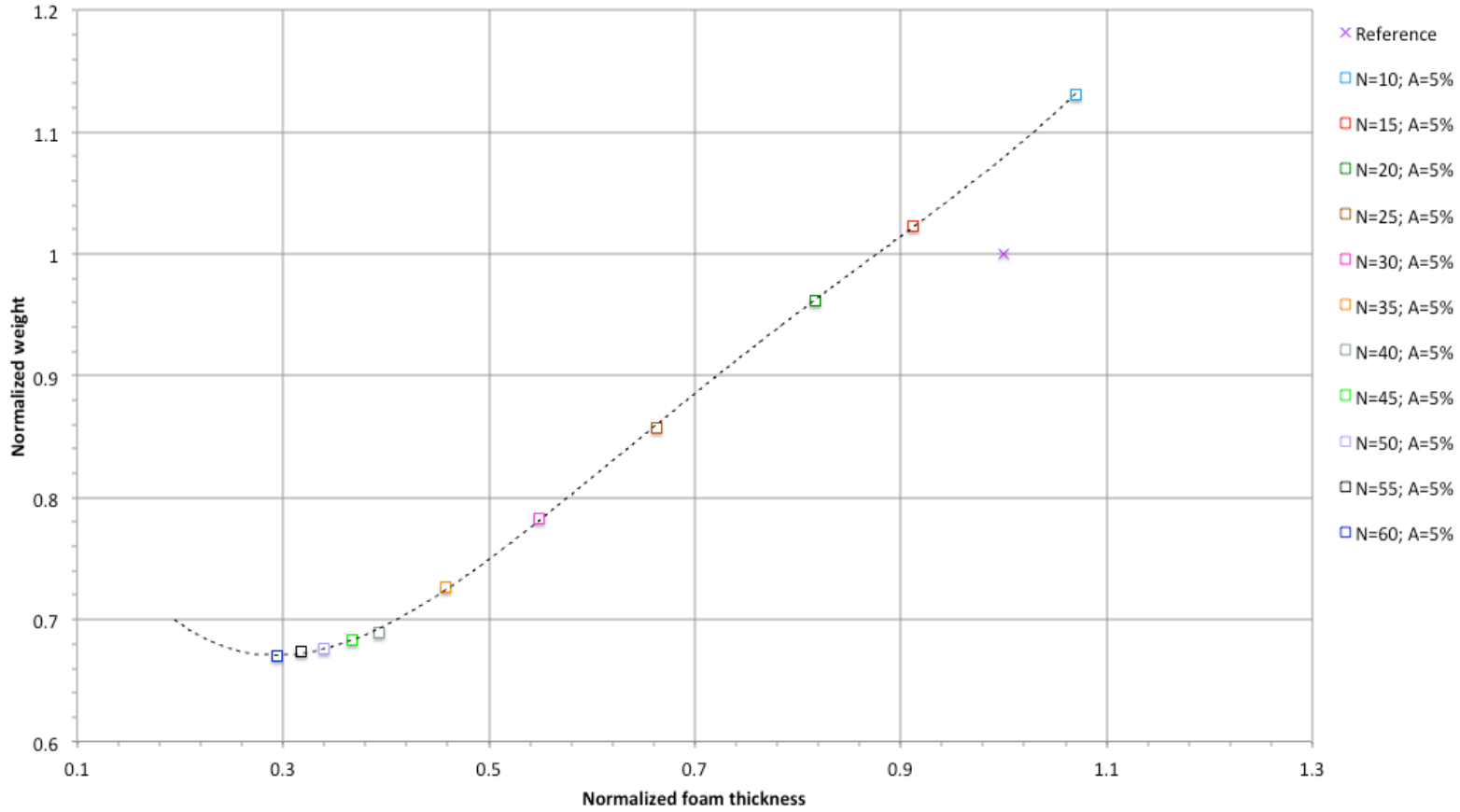

Figure 3.16 Normalized weight vs normalized thickness for A=5%

CHAPTER 4
RESULTS AND DISCUSSION

4.1 Reduced weight configuration for corrugated duct at sea level

The corrugated sandwich composite converging duct gave a significantly better result when compared to a smooth sandwich composite converging duct. For a $[90_2/F/90_2]$ layup, the smooth converging duct gave a minimum weight of 1959.99 kgf for a foam thickness (t_f) of 17.48 mm. For the same layup with same operating conditions, the corrugated converging duct having 60 waves and 5% amplitude gave a reduced weight of 1314.75 kgf for a foam thickness of 5.158 mm. The weight of the corrugated duct was 32% less than that of the smooth converging duct. The foam thickness required to design the corrugated duct was 70% less than the foam thickness required for a smooth duct.

As observed in Figure 4.2, the configurations for A=5% seem to approach a shallow minimum i.e. the reduction in weight is smaller when compared to the previous configuration. Upon comparing the configurations for A=5% involving N=50; and N=55, the reduction in weight was 0.6% for a 6% reduction in foam thickness. For a similar comparison for A=5% involving N=55 and N=60, we obtain a 0.4% reduction in weight for 7% reduction in foam thickness. Based on the response observed in Figure 3.16 it is likely the weight of the corrugated duct may increase with a further increase in number of waves.

The computational effort required to perform analysis involving high number of waves was challenging. Due to the time constraints configurations involving a higher number of waves than N=60 for A=5% were not investigated. Considering the case of smooth duct, it can be represented as A=0 with N taking any value which gives a weight of 1959.99 kgf. Hence it might be of interest to investigate configurations involving an amplitude of corrugation lower than A=5% to capture the behavior of corrugated duct.

Table 4.1 Reduced weight of corrugated configurations at sea level

Number of waves	**Amplitude (%r_i)**	**Foam thickness (mm)**	**Weight (kgf)**
10	5	1.070	1.131
	10	0.953	1.099
	15	0.926	1.148
15	5	0.912	1.022
	10	0.750	0.971
	15	0.755	1.070
20	5	0.816	0.962
	7	0.676	0.888
	12	0.667	0.988
	15	0.708	1.108
25	5	0.662	0.857
	7	0.563	0.820
	10	0.612	0.937
30	5	0.548	0.783
	6	0.498	0.765
	7	0.487	0.781
	8	0.531	0.847
	10	0.564	0.942
35	5	0.458	0.726
40	5	0.393	0.689
45	5	0.367	0.683
50	5	0.339	0.675
55	5	0.317	0.673
60	5	0.294	0.670

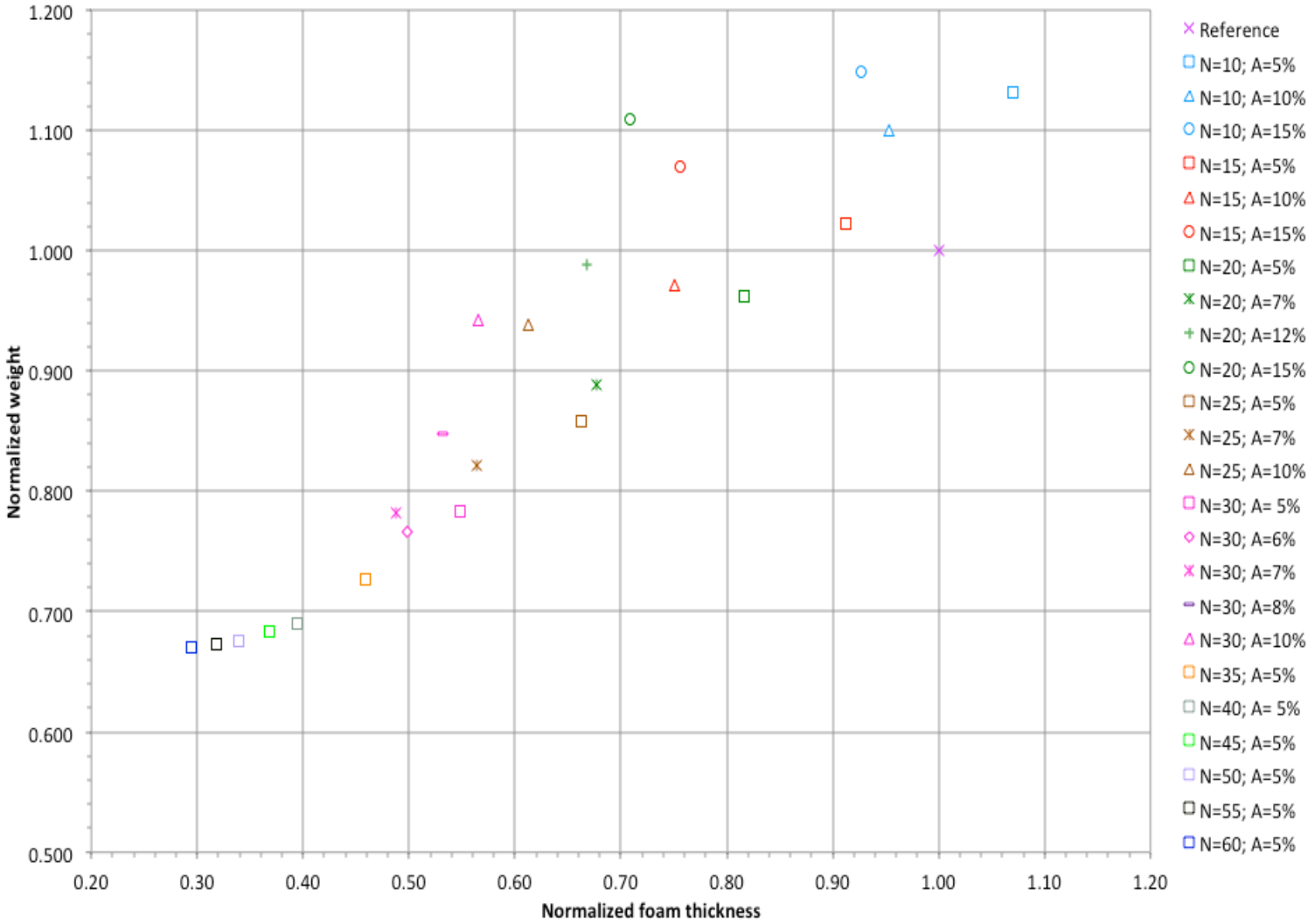

Figure 4.1 Weight of optimized corrugated configurations as function of foam thickness for [90_2/F/90_2]

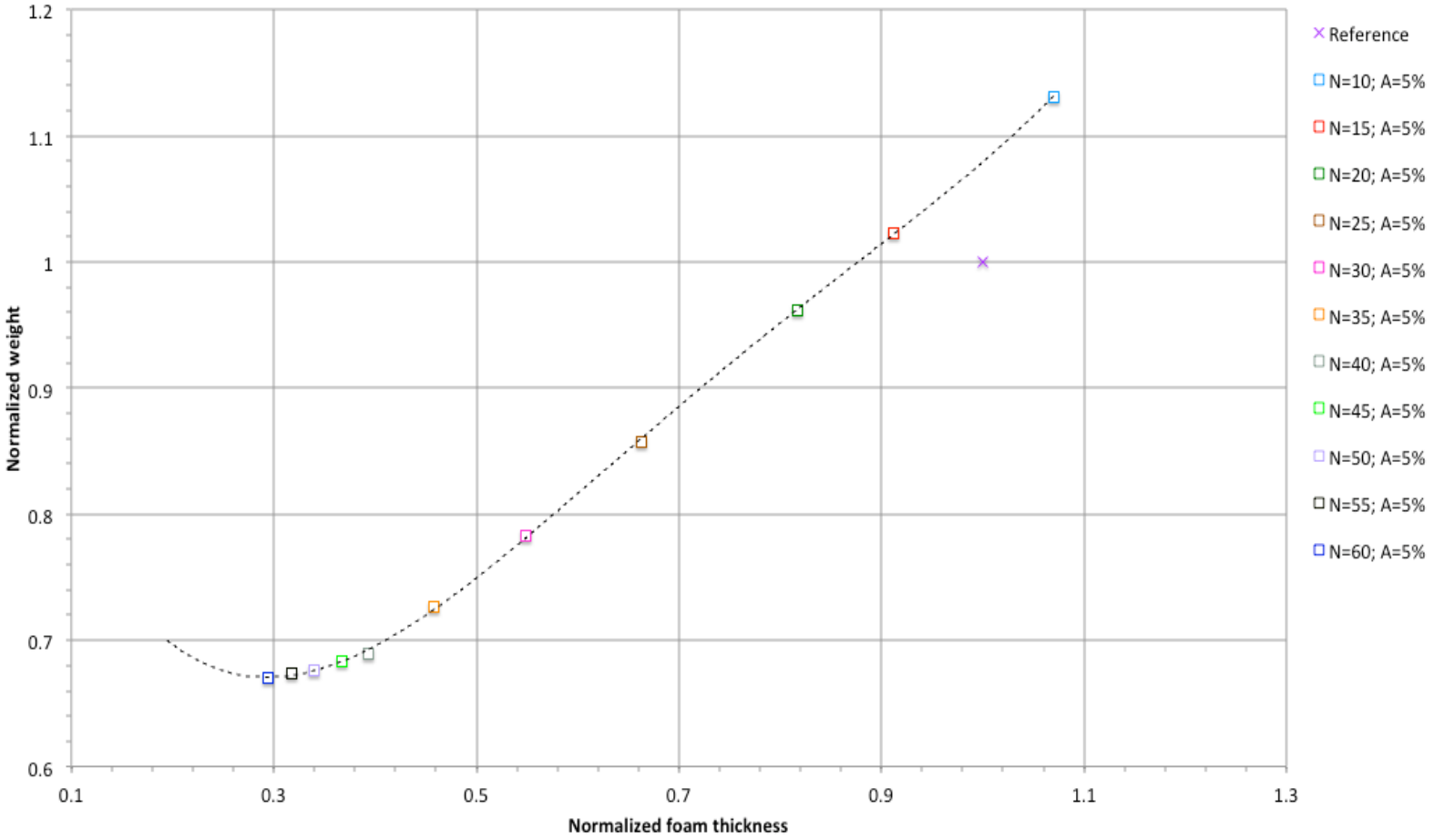

Figure 4.2 Weight of corrugated configuration for A=5%

CHAPTER 5
CONCLUSION AND RECOMMENDATIONS

5.1 Conclusion

The weight reduction analysis of a corrugated sandwich composite duct subjected to stability constraints under lateral pressure yielded a positive result. It was observed that as the amplitude of wave varied for a certain number of corrugation waves the required foam thickness also varied. As the number of waves increased, it was observed that the most reduced weight configuration was achieved at lower amplitude. The weight of the duct is the sum of the weight of the facesheets and the foam. Higher amplitudes corresponded with higher areas, which would affect the weight conversely even if there were a decrease in foam thickness. Based on this observation, an approach involving higher number of waves and lower amplitude was adopted to achieve the reduced weight for the corrugated duct. The reduced weight for a corrugated duct at sea level with 50% margin of safety observed was achieved at A=5% with N=60. This is not the global minimum as we can see in Figure 5.2 the curve for A=5% has a shallow minimum trend. As the computational time required was higher for configurations involving high number of waves or large amplitudes, it was not possible to investigate configurations involving lower amplitudes than A=5%.

5.2 Recommendations

1. To verify the accuracy of FEM results an experimental investigation could be conducted.
2. Analysis should be also performed for operating conditions at altitudes of 32 kft and 65 kft.
3. Practical layup should be considered in order to avoid delamination or fiber splitting.
4. Configurations involving amplitudes less than A=5% should be investigated

REFERENCES

[1] Meier, G. E. A., Suryanarayana, G. K., and Pauer, H., and, "Bluff-Body Drag Reduction by Passive Ventilation," *Experiments in Fluids*, 16, 1993, pp 73-81,

[2] Dancila, D. S., "Advanced Airship Technologies," US Patent 8342442, January 2013

[3] Khode, U., "Finite Element Based Stability-Constrained Weight Minimization of Sandwich Composite Ducts for Airship Applications," MS Thesis UT Arlington, July 2011

[4] Hao, B., Cho, C., and Lee, S.W.," Buckling and Postbuckling of Soft-core Sandwich Plates with Composite Facesheets," SpringerLink, *Computational Mechanics* 25, 2000, pp 421-429

[5] Leishman, J.G.," Principles of Helicopter Aerodynamics," Cambridge University Press, New York, 2006.

[6] ABAQUS v6.14 Reference Manual

[7] Weingarten, V, I., Seide, P., Petersen, J. P., "Buckling of Thin Walled Circular Cylinders," NASA SP-8007, 1968

APPENDIX A

CALCULATION OF REQUIRED THICKNESS

To determine the interpolation function, three initial guesses were made. These three points were used to determine a quadratic function for the factor of safety, which was solved for required foam thickness for a factor of safety of 1.5.

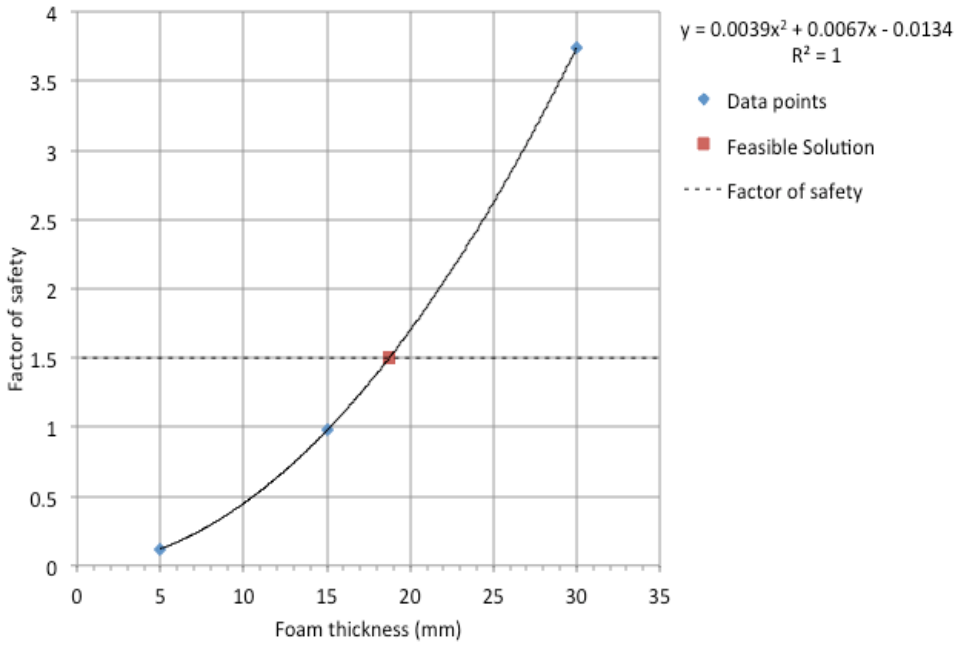

Figure A.1 Factor of safety as a function of foam thickness for [90_2/F/90_2] with N=10, A=5% configuration

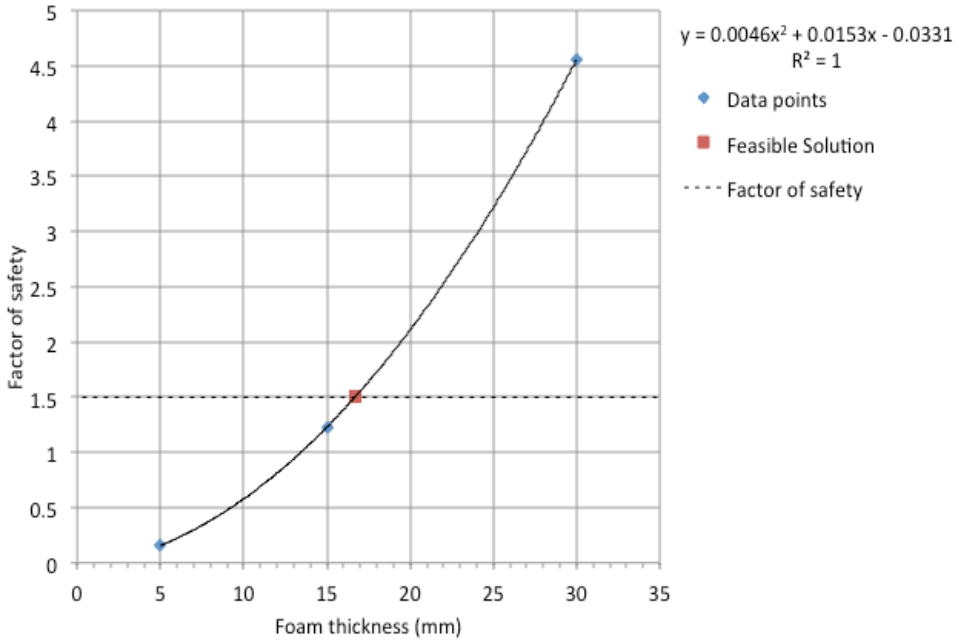

Figure A.2 Factor of safety as a function of foam thickness for $[90_2/F/90_2]$ with N=10; A=10%

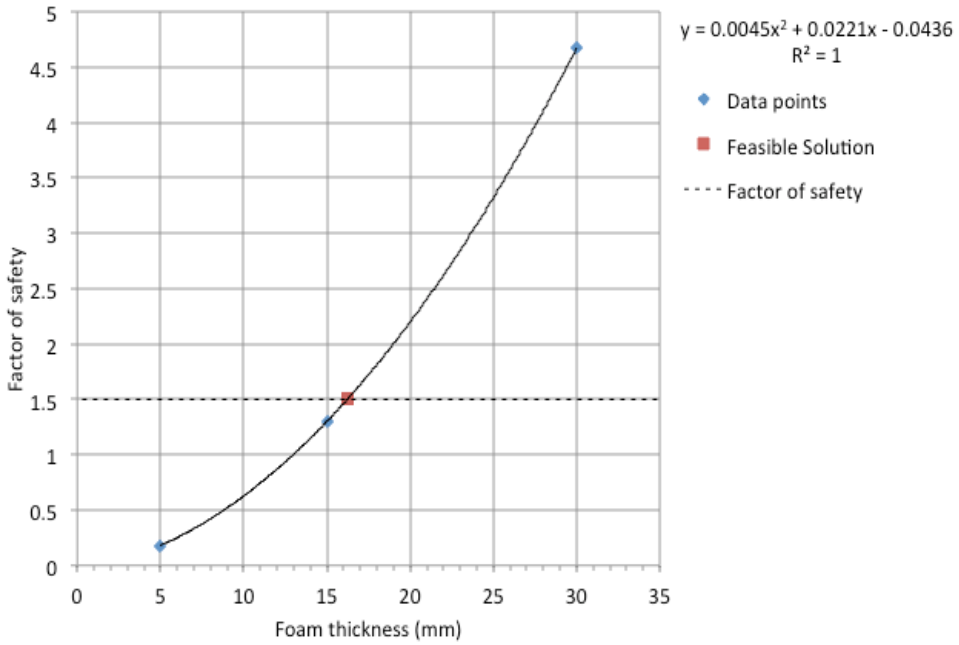

Figure A.3 Factor of safety as a function of foam thickness for $[90_2/F/90_2]$ with N=10; A=15% configuration

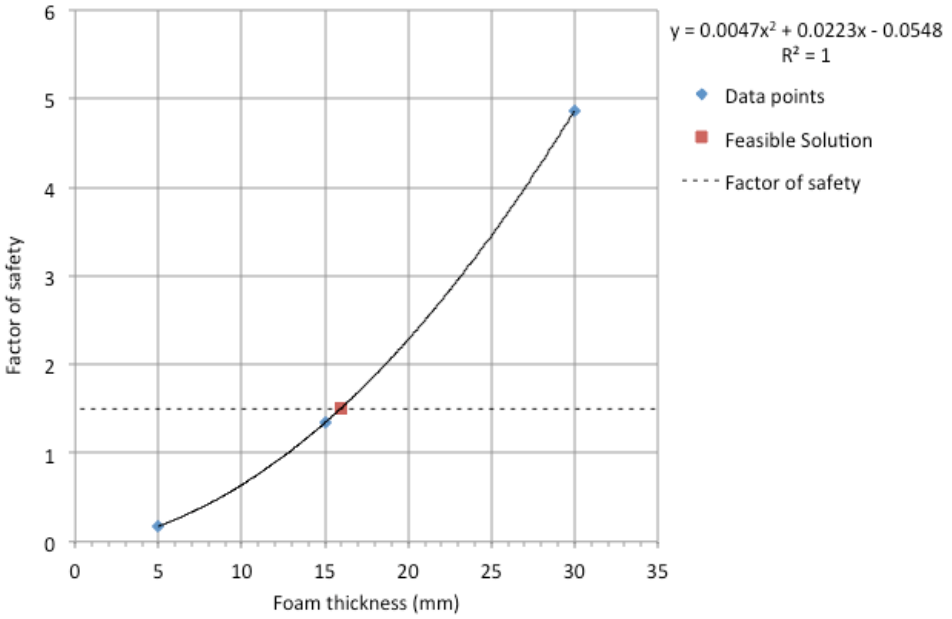

Figure A.4 Factor of safety as a function of foam thickness for [90_2/F/90_2] with N=15; A=5% configuration

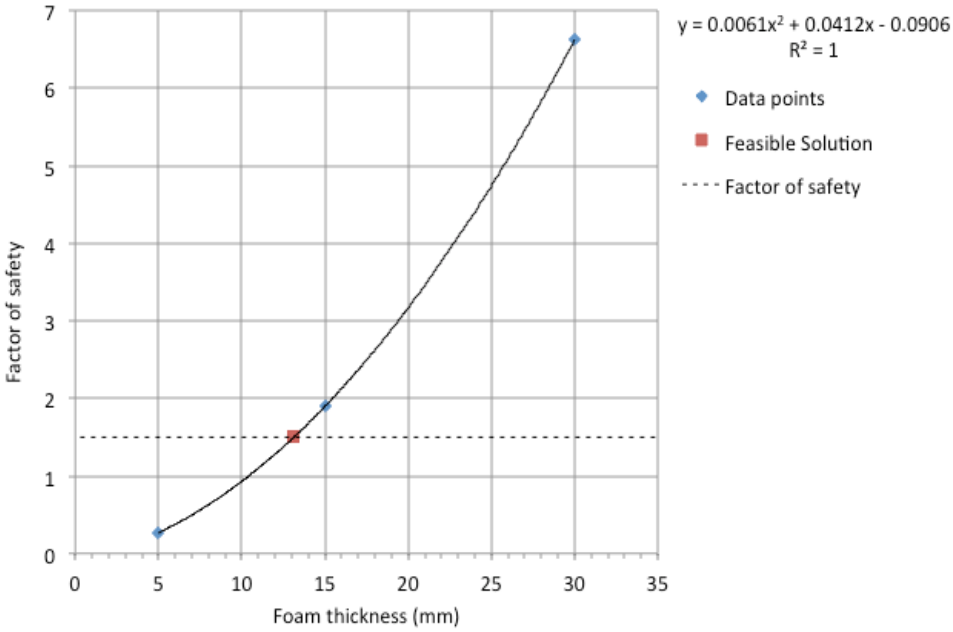

Figure A.5 Factor of safety as a function of foam thickness for [90_2/F/90_2] with N=15; A=10% configuration

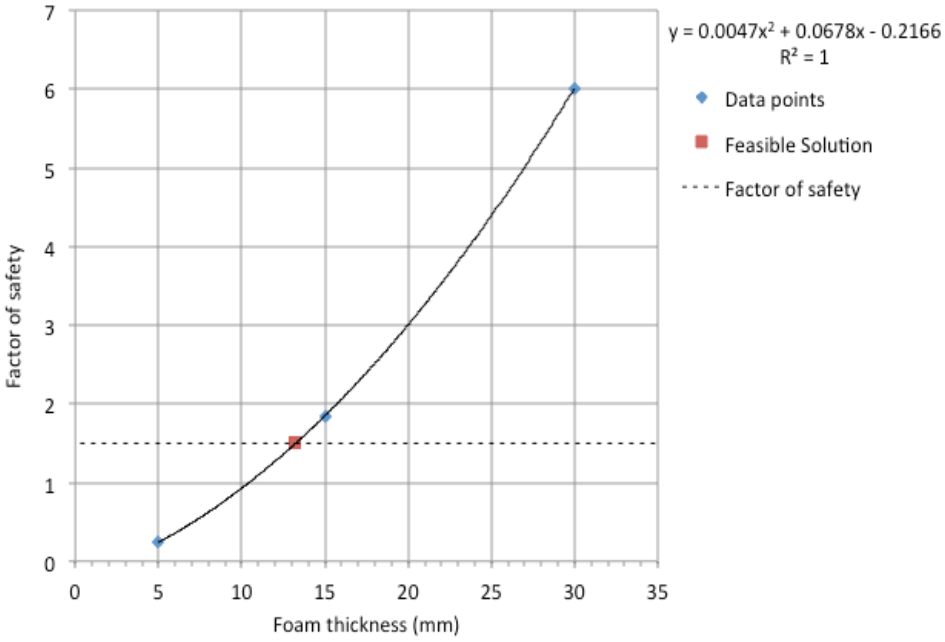

Figure A.6 Factor of safety as a function of foam thickness for [90_2/F/90_2] with N=15; A=15% configuration

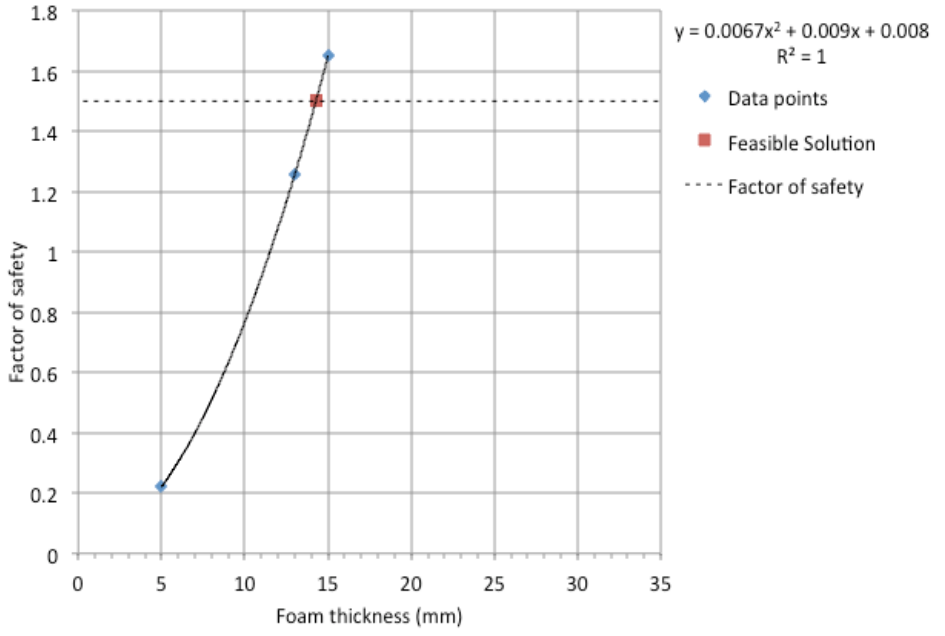

Figure A.7 Factor of safety as a function of foam thickness for [90_2/F/90_2] with N=20; A=5% configuration

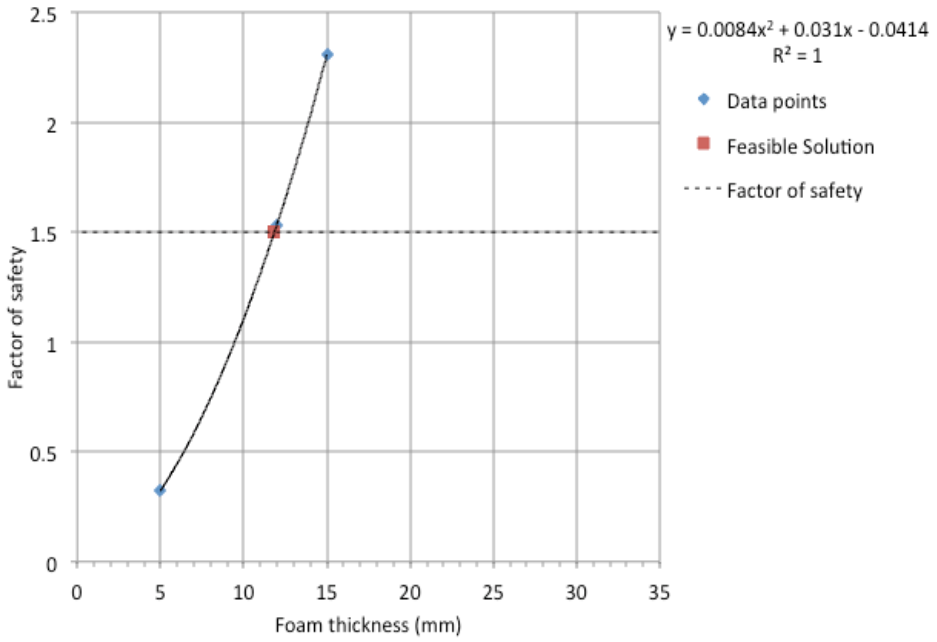

Figure A.8 Factor of safety as a function of foam thickness for [90_2/F/90_2] with N=20; A=7% configuration

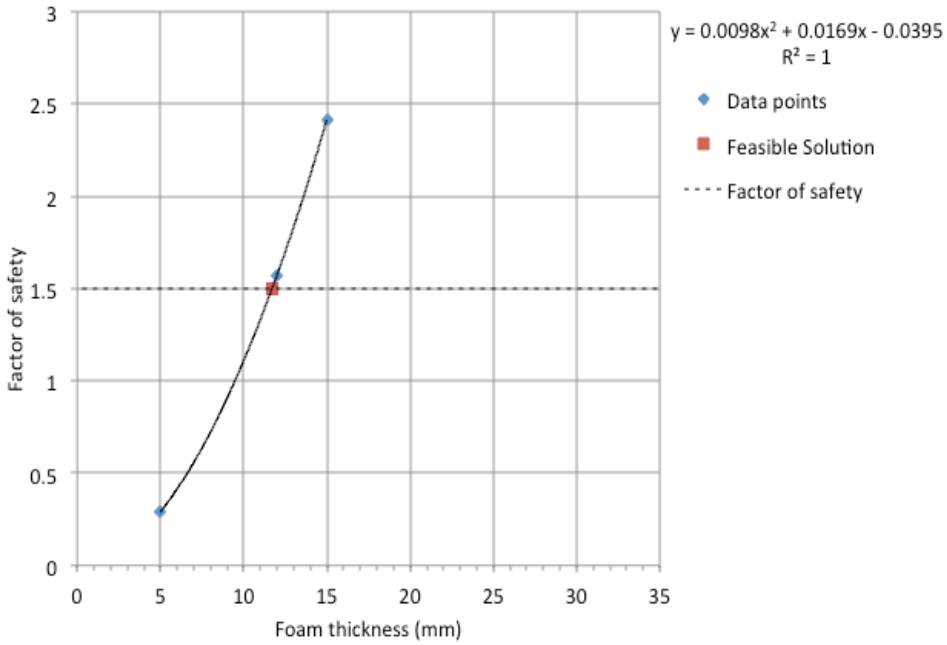

Figure A.9 Factor of safety as a function of foam thickness for [90_2/F/90_2] with N=20; A=12% configuration

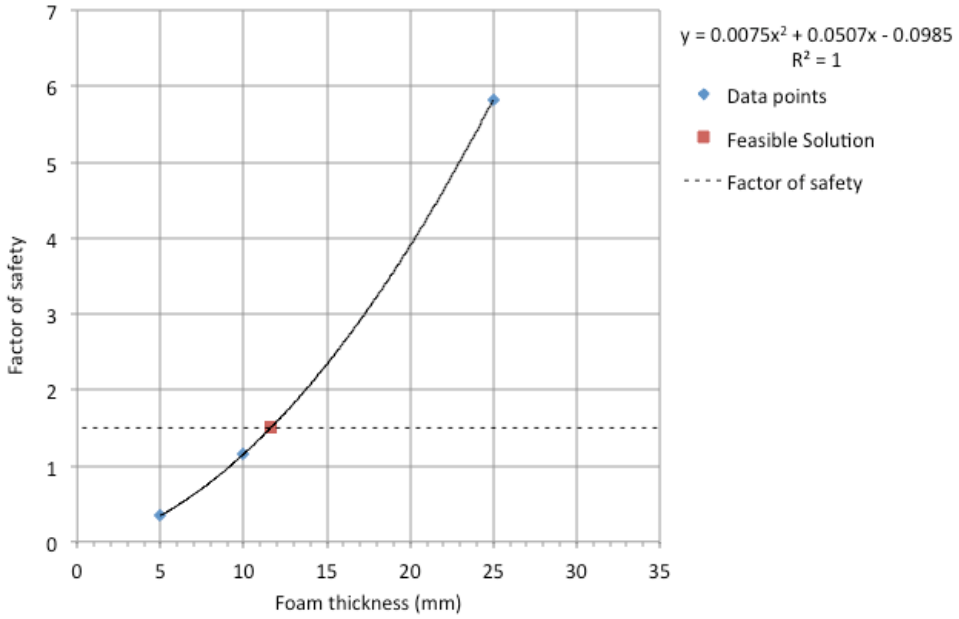

Figure A.10 Factor of safety as a function of foam thickness for [90_2/F/90_2] with N=25; A=5% configuration

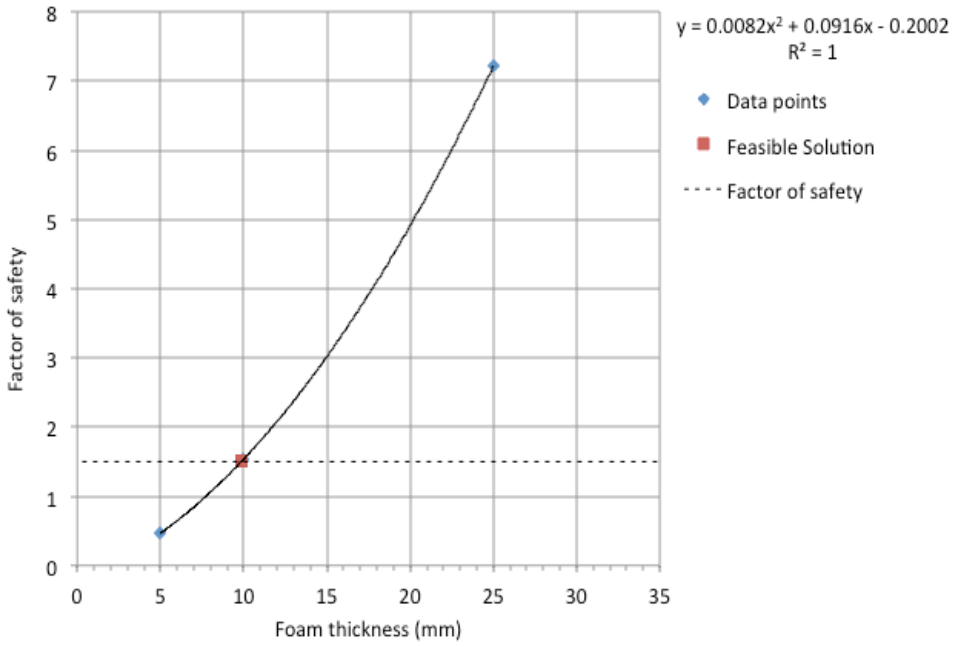

Figure A.11 Factor of safety as a function of foam thickness for [90_2/F/90_2] with N=25; A=7% configuration

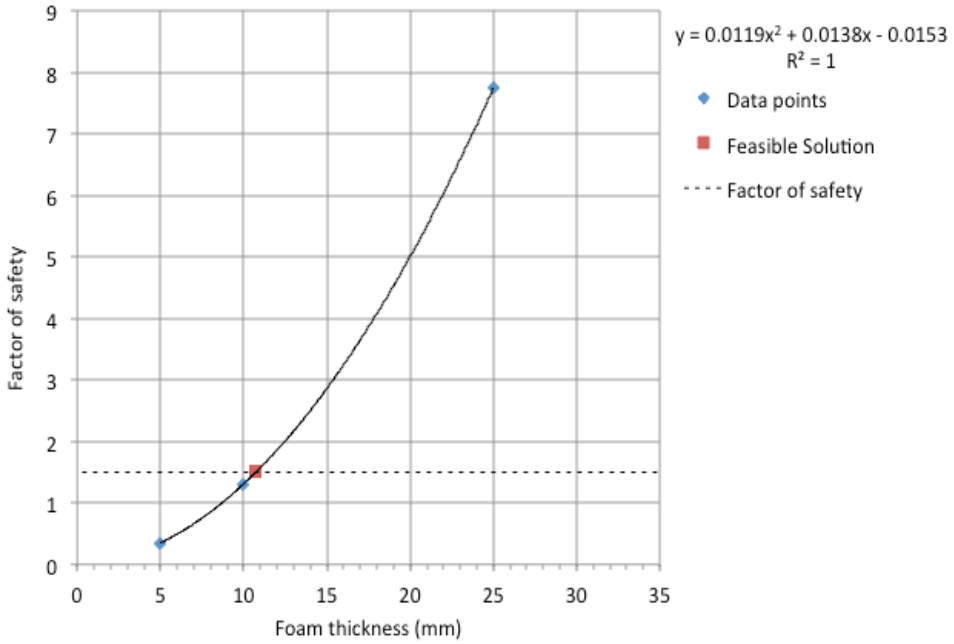

Figure A.12 Factor of safety as a function of foam thickness for [90_2/F/90_2] with N=25; A=10% configuration

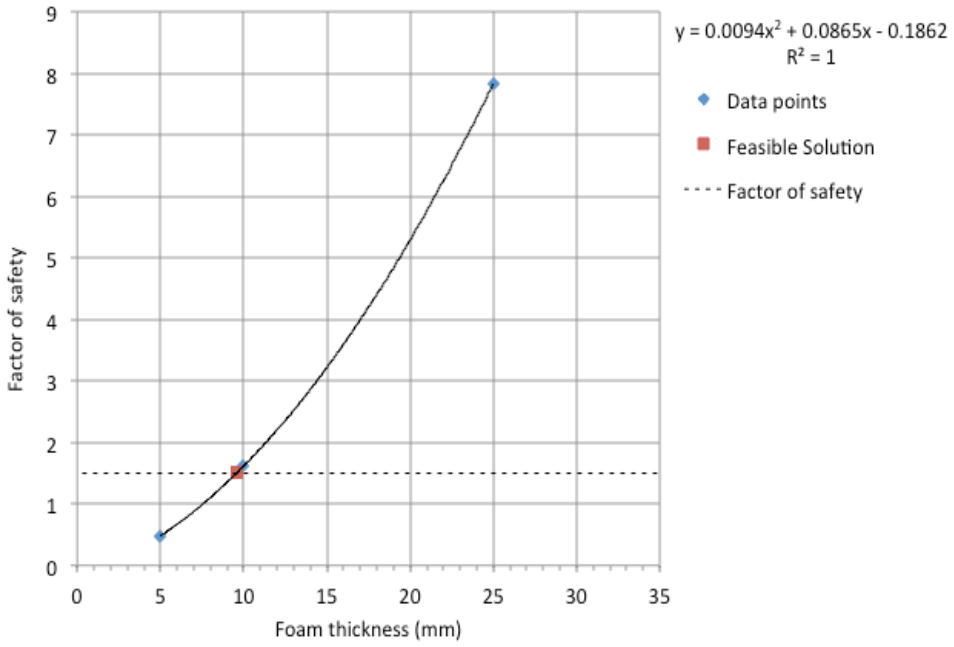

Figure A.13 Factor of safety as a function of foam thickness for [90_2/F/90_2] with N=30; A=5% configuration

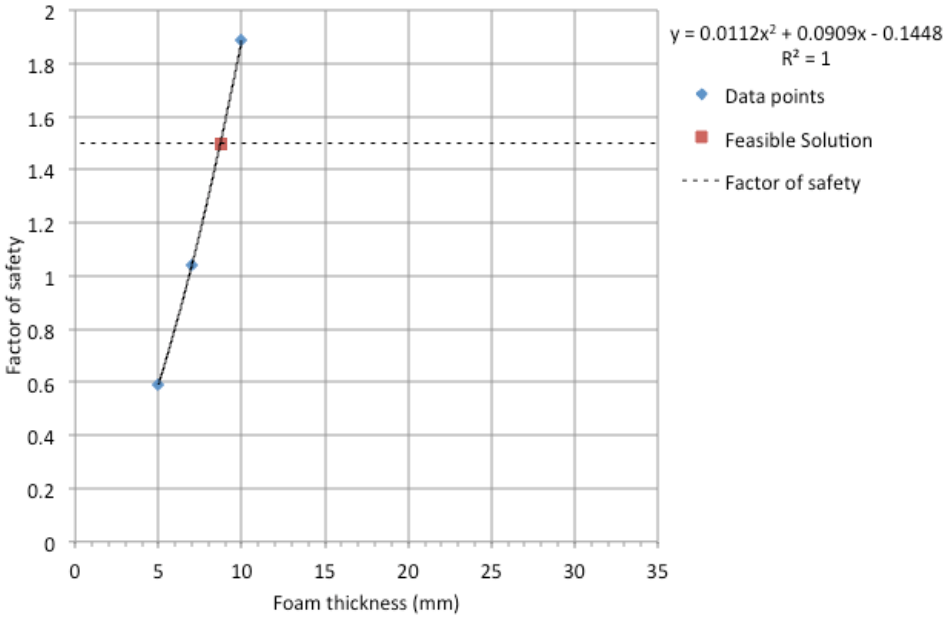

Figure A.14 Factor of safety as a function of foam thickness for [90_2/F/90_2] with N=30; A=6% configuration

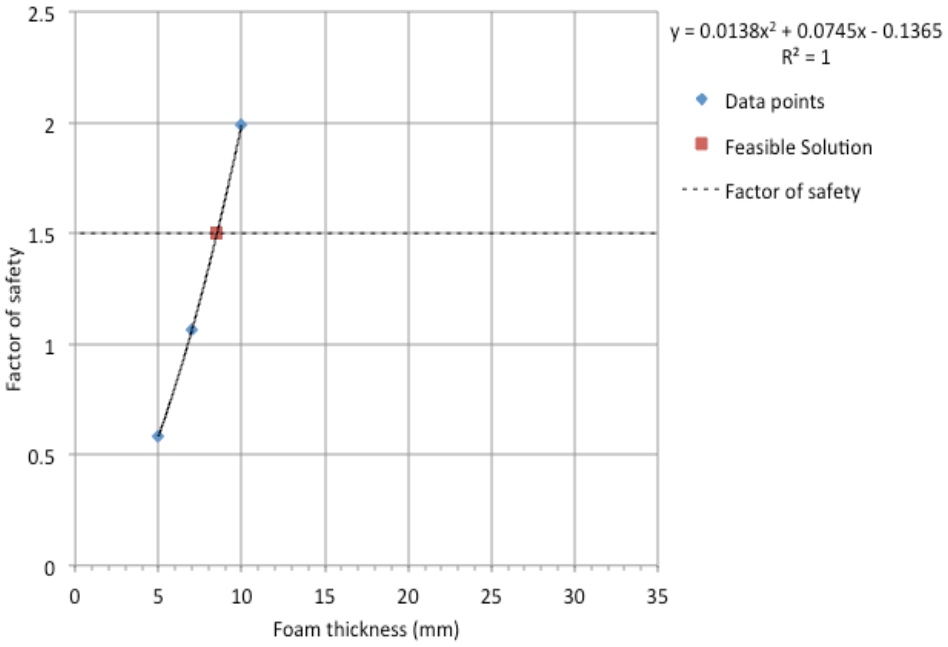

Figure A.15 Factor of safety as a function of foam thickness for [90_2/F/90_2] with N=30; A=7% configuration

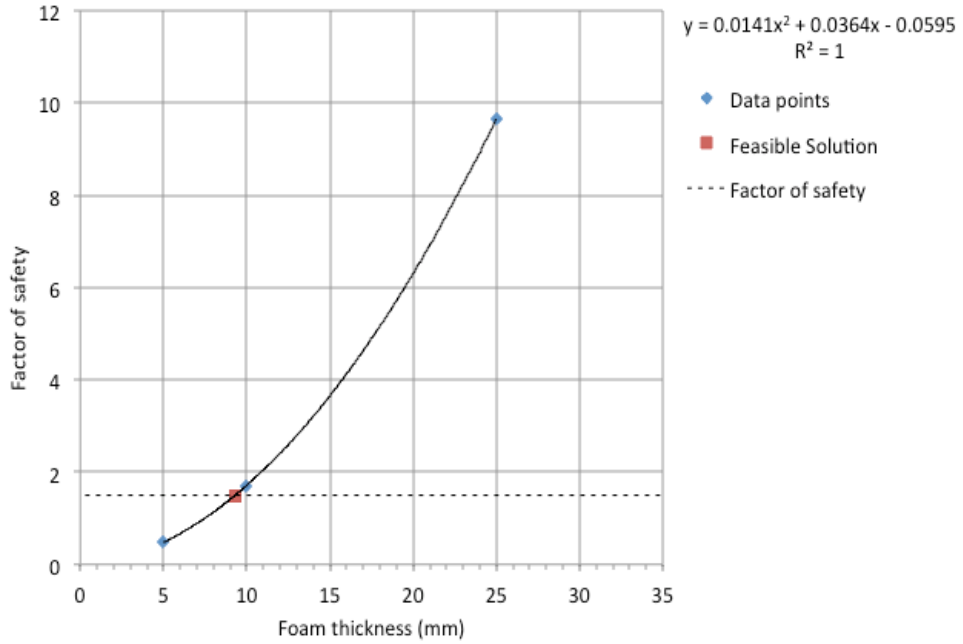

Figure A.16 Factor of safety as a function of foam thickness for [90_2/F/90_2] with N=30; A=8% configuration

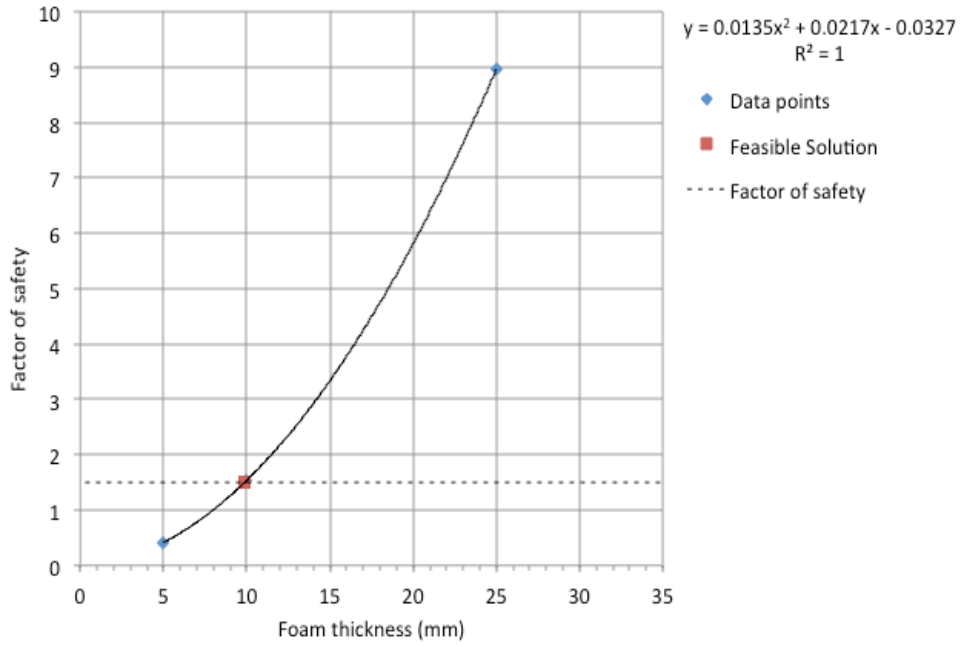

Figure A.17 Factor of safety as a function of foam thickness for [90_2/F/90_2] with N=30; A=10% configuration

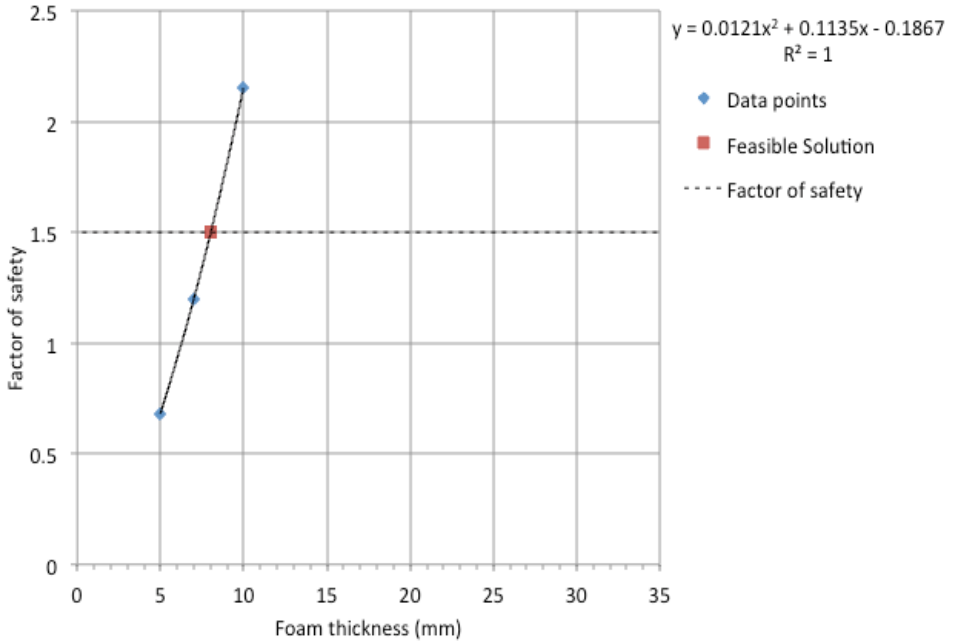

Figure A.18 Factor of safety as a function of foam thickness for [90_2/F/90_2] with N=35; A=5% configuration

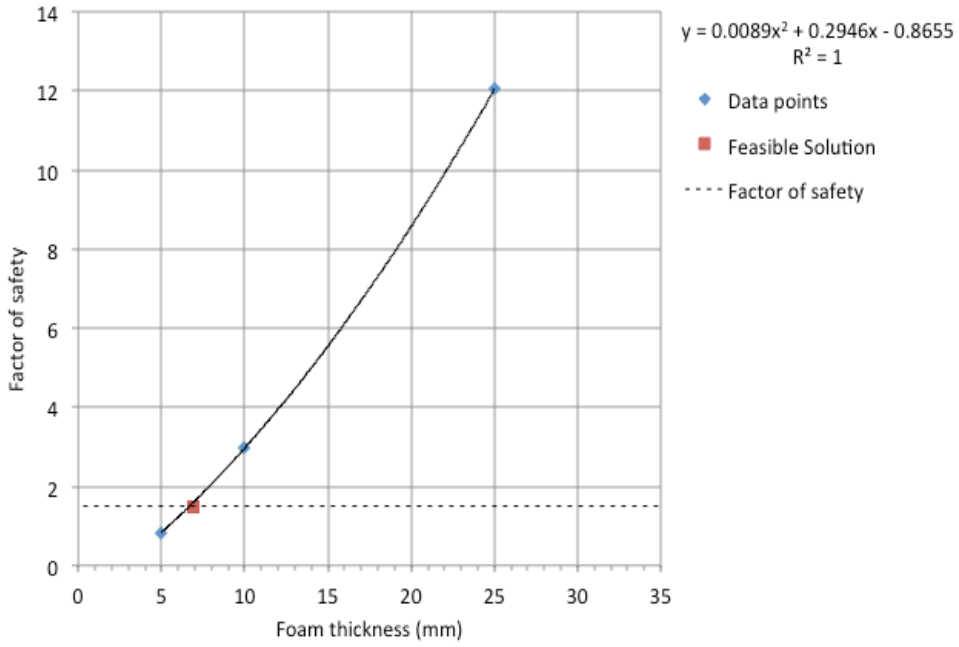

Figure A.19 Factor of safety as a function of foam thickness for [90_2/F/90_2] with N=40; A=5% configuration

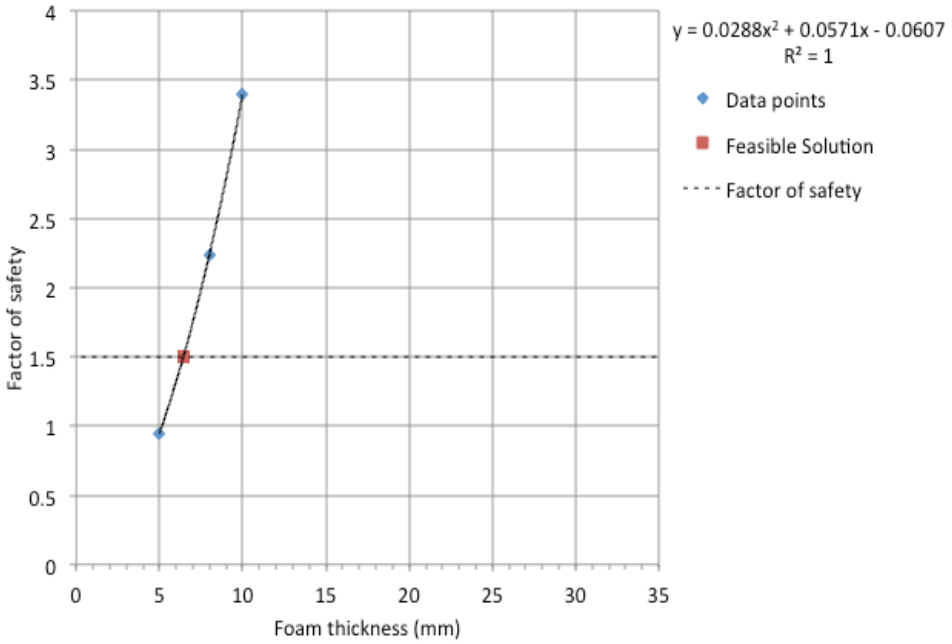

Figure A.20 Factor of safety as a function of foam thickness for [90_2/F/90_2] with N=45; A=5% configuration

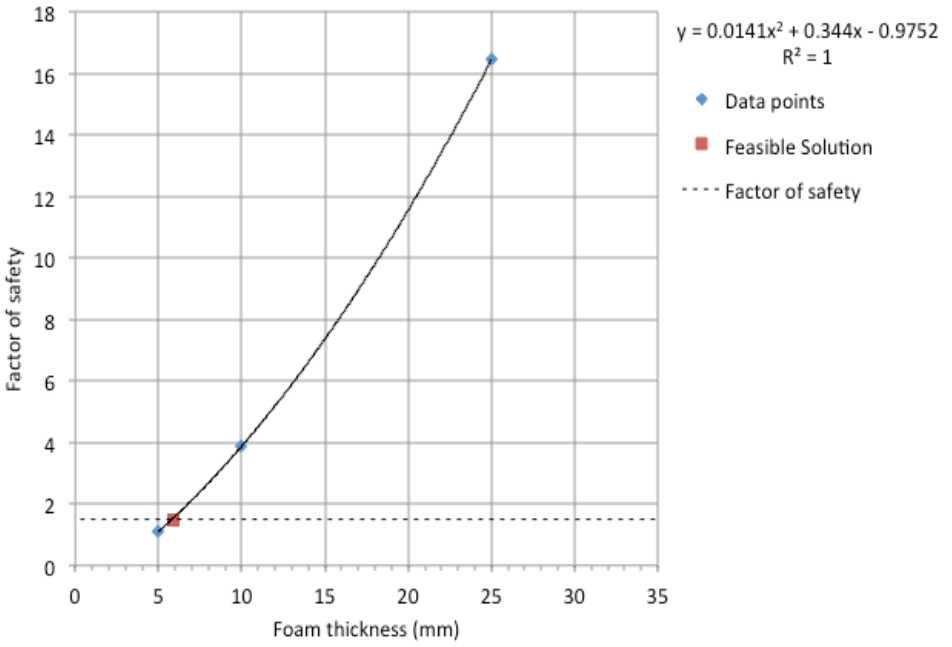

Figure A.21 Factor of safety as a function of foam thickness for [90_2/F/90_2] with N=50; A=5% configuration

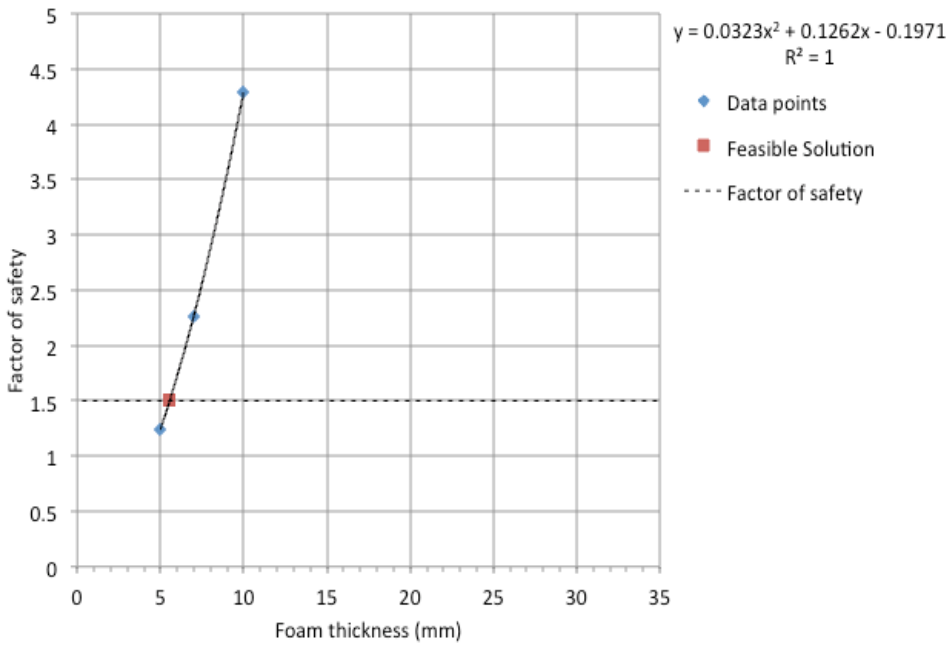

Figure A.22 Factor of safety as a function of foam thickness for [90_2/F/90_2] with N=55; A=5% configuration

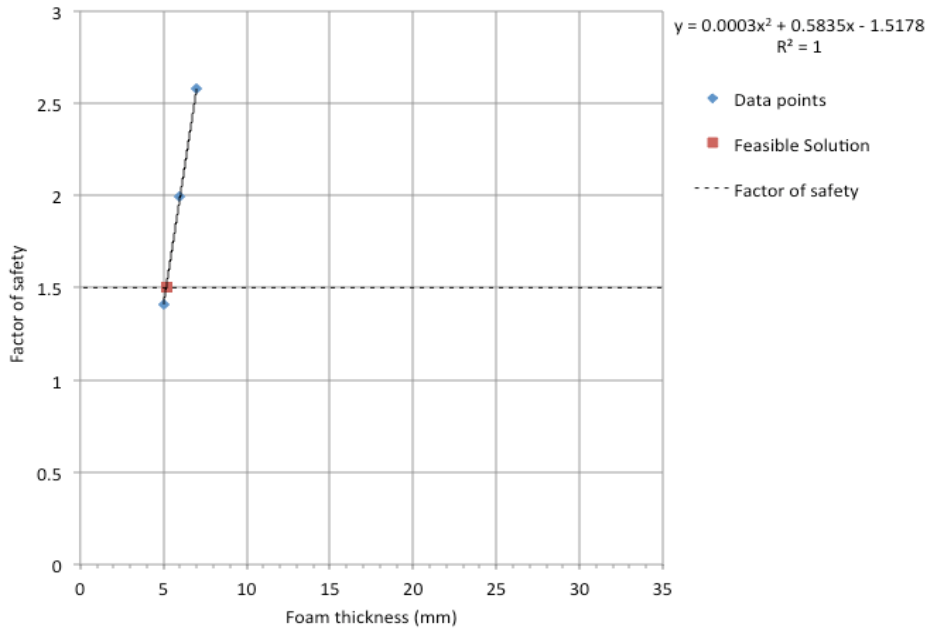

Figure A.23 Factor of safety as a function of foam thickness for [90_2/F/90_2] with N=60; A=5% configuration

BIOGRAPHICAL INFORMATION

Soham Umbrajkar is currently a PhD student in Mechanical Engineering at The University of Texas at Arlington. In May 2014, he graduated with a Bachelor of Engineering degree in Mechanical Engineering from the University of Mumbai, Mumbai, India. Due to his interest in solid mechanics and structures, he joined The University of Texas at Arlington as a graduate student in Mechanical Engineering, earning a Master of Science degree in May 2016.